Confinement-induced p-wave resonances from s-wave interactions

Citation: Nishida, Yusuke, and Shina Tan. "Confinement-induced P-wave Resonances from S-wave Interactions." Physical Review A 82.6 (2010) : 062713. © 2010 The American Physical Society

As Published: http://dx.doi.org/10.1103/PhysRevA.82.062713

Publisher: American Physical Society

Persistent URL: http://hdl.handle.net/1721.1/63129

Version: Final published version: final published article, as it appeared in a journal, conference proceedings, or other formally published context

Confinement-induced *p*-wave resonances from *s*-wave interactions

Yusuke Nishida[1] and Shina Tan[2,3]

[1]*Center for Theoretical Physics, Massachusetts Institute of Technology, Cambridge, Massachusetts 02139, USA*

[2]*Department of Physics, Yale University, New Haven, Connecticut 06520, USA*

[3]*School of Physics, Georgia Institute of Technology, Atlanta, Georgia 30332, USA*

(Received 30 October 2010; published 27 December 2010)

We show that a purely *s*-wave interaction in three dimensions (3D) can induce higher partial-wave resonances in mixed dimensions. We develop two-body scattering theories in all three cases of 0D-3D, 1D-3D, and 2D-3D mixtures and determine the positions of higher partial-wave resonances in terms of the 3D *s*-wave scattering length assuming a harmonic confinement potential. We also compute the low-energy scattering parameters in the *p*-wave channel (scattering volume and effective momentum) that are necessary for the low-energy effective theory of the *p*-wave resonance. We point out that some of the resonances observed in the Florence group experiment [Phys. Rev. Lett. **104**, 153202 (2010)] can be interpreted as the *p*-wave resonances in the 2D-3D mixed dimensions. Our study paves the way for a variety of physics, such as Anderson localization of matter waves under *p*-wave resonant scatterers.

DOI: 10.1103/PhysRevA.82.062713 PACS number(s): 34.50.−s

I. INTRODUCTION

Scattering resonances play a central role in cold-atom physics [1]. In particular, *s*-wave Feshbach resonances induced by a magnetic field have been utilized to control the atom-atom interaction and have led to experimental realization of a rich variety of physics, such as the BCS-BEC crossover in Fermi gases [2–4]. Although a *p*-wave analog of the BCS-BEC crossover has been predicted theoretically [5–9] and *p*-wave and higher partial-wave resonances have been observed experimentally [1,10–19], *p*-wave superfluids have not been realized in cold-atom experiments so far. This is because Fermi gases in the vicinity of the *p*-wave Feshbach resonances are unstable owing to inelastic collisions decaying into deeply bound dimers and do not reach their equilibrium within their short lifetime [20,21]. In contrast, Fermi gases in the vicinity of the *s*-wave Feshbach resonances are long lived because such inelastic collisions are strongly suppressed by the Pauli exclusion principle [22].

In this paper, we propose a way to induce *p*-wave and higher partial-wave resonances from the *s*-wave Feshbach resonance only. This can be achieved by using a mixture of two atomic species A and B in mixed dimensions, where A atoms are confined in lower dimensions [quasi-zero dimension (0D), one dimension (1D), or two dimensions (2D)] and interact with B atoms living in three dimensions (3D) [23,24] (see Fig. 1). Indeed, the authors of Ref. [23] mention the possibility of *p*-wave resonances in the 0D-3D mixture. Higher partial-wave resonances induced from a purely *s*-wave interaction seem counterintuitive but can be understood by generalizing the argument for *s*-wave resonances given in Ref. [23].

Suppose an *s*-wave interspecies interaction between A and B atoms supports a bound state with its binding energy $E_b < 0$. We confine only the A atom by a 3D harmonic potential with the oscillator frequency ω. Because the AB molecule also feels the confinement potential, its center-of-mass motion is quantized. In the limit $|E_b| \gg \hbar\omega$ or $m_A \gg m_B$, the energy of the AB molecule E_{AB} is given by a sum of its center-of-mass energy and binding energy:

$$E_{AB} = \left(\frac{3}{2} + \ell + 2n\right)\sqrt{\frac{m_A}{m_A + m_B}}\hbar\omega - |E_b|, \qquad (1)$$

where m_A (m_B) is the mass of the A (B) atom, $\ell = 0,1,2,\ldots$ is an orbital angular momentum quantum number, and $n \geqslant 0$ is an integer. We can view these quantized energy levels as a tower of ℓth partial-wave "Feshbach molecules." When one of them coincides with the A-B scattering threshold at $\frac{3}{2}\hbar\omega$, the coupling between the center-of-mass and relative motions leads to the resonance occurring in the ℓth partial-wave channel. Furthermore, there exists a series of resonances in each partial-wave channel corresponding to different values of n.

Similarly, in the 1D-3D mixture, the A atom is confined by a 2D harmonic potential and the energy of the AB molecule is quantized as

$$E_{AB} = (1 + |m| + 2n)\sqrt{\frac{m_A}{m_A + m_B}}\hbar\omega - |E_b|, \qquad (2)$$

where $m = 0, \pm 1, \pm 2, \ldots$ is a magnetic quantum number. When one of them coincides with the A-B scattering threshold at $\hbar\omega$, the resonance occurs in the $|m|$th partial-wave channel. There exists a series of resonances in each partial-wave channel corresponding to different values of n.

In the 2D-3D mixture, the A atom is confined by a 1D harmonic potential and the energy of the AB molecule is

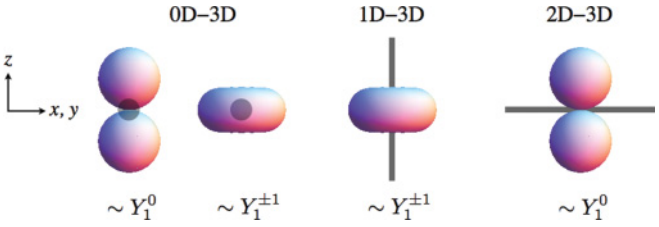

FIG. 1. (Color online) Illustrations of shallow *p*-wave molecules in mixed dimensions. Shown are the asymptotic angular wave functions of B atoms in 3D relative to A atoms confined in 0D (origin), 1D (z axis), and 2D (xy plane), respectively. See the text for details.

quantized as

$$E_{AB} = \left(\frac{1}{2} + n\right)\sqrt{\frac{m_A}{m_A + m_B}}\hbar\omega - |E_b|. \tag{3}$$

When one of them coincides with the A-B scattering threshold at $\frac{1}{2}\hbar\omega$, the resonance occurs. Because the wave function of the $A\bar{B}$ molecule has the even (odd) parity for an even (odd) n, the associated resonance is in the even (odd)-parity channel, which is also phrased as an s-wave (p-wave) resonance in the 2D-3D mixture. There exists a series of resonances in each parity channel corresponding to different values of n. In order to achieve these higher partial-wave resonances in mixed dimensions, one needs to apply a strong optical lattice only on A atoms without affecting B atoms [25]. Such a species-selective optical lattice has been successfully implemented in a Bose-Bose mixture of ^{41}K and ^{87}Rb [26] and the 2D-3D mixed dimensions have been realized in the Florence group experiment [27].

The above simple arguments illustrate how the higher partial-wave resonances are induced in mixed dimensions from the purely s-wave interaction in a free space. In this paper, we develop two-body scattering theories in mixed dimensions, assuming the harmonic confinement potential and the short-range interspecies interaction characterized by an s-wave scattering length ($\equiv a_{3D}$) and effective range ($\equiv r_{3D}$), which are extensions of analyses in Refs. [23] and [24] aimed for s-wave scatterings only. The two-body scattering of a 0D, 1D, or 2D atom with a 3D atom is three-dimensional in the sense that it is described by three relative coordinates, and thus such scattering theories can be developed in parallel with the ordinary scattering theory in 3D. In particular, we determine the positions of all partial-wave resonances and will see that they are well understood from the above simple arguments in a wide range of the mass ratio $m_A/m_B \gtrsim 1$. We also compute the low-energy scattering parameters in the p-wave channel (scattering volume and effective momentum) that are necessary for the low-energy effective theory of the p-wave resonance in mixed dimensions.

Our analyses and results for the 0D-3D, 1D-3D, and 2D-3D mixtures are presented in Secs. II, III, and IV, respectively, while some details are shown in Appendixes A, B, and C, respectively. Also in Sec. IV, we point out that some of the resonances observed in the Florence group experiment [27] can be interpreted as the p-wave resonances in the 2D-3D mixed dimensions. Finally, Sec. V is devoted to a summary of this paper, and the stability of confinement-induced molecules and their analogy with Kaluza-Klein modes in extra-dimension models are discussed.

For later use, we define the reduced mass $m_{AB} \equiv m_A m_B/(m_A + m_B)$, the total mass $M \equiv m_A + m_B$, and the harmonic oscillator length $l_{\rm ho} \equiv \sqrt{\hbar/m_A\omega}$. Below we set $\hbar = 1$ and the range of integrations is assumed to be from $-\infty$ to ∞ unless otherwise specified.

II. 0D-3D MIXED DIMENSIONS

A. Scattering theory [23]

The scattering of a quasi-0D A atom with a B atom in 3D is described by a Schrödinger equation,

$$\left(-\frac{\nabla_{\boldsymbol{r}_A}^2}{2m_A} + \frac{1}{2}m_A\omega^2\boldsymbol{r}_A^2 - \frac{\nabla_{\boldsymbol{r}_B}^2}{2m_B}\right)\psi(\boldsymbol{r}_A,\boldsymbol{r}_B) = E\psi(\boldsymbol{r}_A,\boldsymbol{r}_B) \tag{4}$$

for $|\boldsymbol{r}_A - \boldsymbol{r}_B| > 0$. The short-range interspecies interaction is implemented by the generalized Bethe-Peierls boundary condition [28,29]:

$$\psi(\boldsymbol{r}_A,\boldsymbol{r}_B)|_{\boldsymbol{r}_A,\boldsymbol{r}_B\to\boldsymbol{r}} \to \left[\frac{1}{\tilde{a}(\hat{E}_c)} - \frac{1}{|\boldsymbol{r}_A - \boldsymbol{r}_B|}\right]\chi(\boldsymbol{r}). \tag{5}$$

Here $\tilde{a}(\hat{E}_c)$ is the energy-dependent "scattering length" defined by

$$\frac{1}{\tilde{a}(\hat{E}_c)} \equiv \frac{1}{a_{3D}} - m_{AB}r_{3D}\hat{E}_c, \tag{6}$$

and the collision energy operator $\hat{E}_c$ in the present case is given by

$$\hat{E}_c = E - \left(-\frac{\nabla_{\boldsymbol{r}}^2}{2M} + \frac{1}{2}m_A\omega^2\boldsymbol{r}^2\right). \tag{7}$$

The solution to the Schrödinger equation (4) can be written as

$$\psi(\boldsymbol{r}_A,\boldsymbol{r}_B) = \psi_0(\boldsymbol{r}_A,\boldsymbol{r}_B) + \frac{2\pi}{m_{AB}}\int d\boldsymbol{r}' G_E(\boldsymbol{r}_A,\boldsymbol{r}_B;\boldsymbol{r}',\boldsymbol{r}')\chi(\boldsymbol{r}'), \tag{8}$$

where ψ_0 is a solution in the noninteracting limit and G_E is the retarded Green's function for the noninteracting Hamiltonian:

$$\begin{aligned} G_E(\boldsymbol{r}_A,\boldsymbol{r}_B;\boldsymbol{r}'_A,\boldsymbol{r}'_B) &\equiv \langle \boldsymbol{r}_A,\boldsymbol{r}_B|\frac{1}{E - H_0 + i0^+}|\boldsymbol{r}'_A,\boldsymbol{r}'_B\rangle \\ &= -\frac{m_B}{2\pi}\sum_{\boldsymbol{n}}\phi_{\boldsymbol{n}}(\boldsymbol{r}_A)\phi^*_{\boldsymbol{n}}(\boldsymbol{r}'_A) \\ &\quad\times\frac{e^{-\sqrt{2m_B}\sqrt{\left(n_x+n_y+n_z+\frac{3}{2}\right)\omega - E - i0^+}|\boldsymbol{r}_B - \boldsymbol{r}'_B|}}{|\boldsymbol{r}_B - \boldsymbol{r}'_B|}. \end{aligned} \tag{9}$$

Here $\phi_{\boldsymbol{n}}$ with quantum numbers $\boldsymbol{n} = (n_x,n_y,n_z)$ is the normalized wave function of an A atom in the 3D harmonic potential.

We now consider the low-energy scattering in which

$$E - \frac{3}{2}\omega \equiv \frac{k^2}{2m_B} \ll \omega \tag{10}$$

is satisfied, and then ψ_0 becomes

$$\psi_0(\boldsymbol{r}_A,\boldsymbol{r}_B) = Ce^{i\boldsymbol{k}\cdot\boldsymbol{r}_B}\phi_{\boldsymbol{0}}(r_A), \tag{11}$$

which represents the A atom in the ground state of the 3D harmonic potential and the plane wave of B atom with the wave vector $\boldsymbol{k}$. The asymptotic form of the wave function at a large distance $|\boldsymbol{r}_B| \gg l_{\rm ho}$ is given by

$$\psi(\boldsymbol{r}_A,\boldsymbol{r}_B) \to C\left[e^{i\boldsymbol{k}\cdot\boldsymbol{r}_B} + \frac{e^{ikr_B}}{r_B}f(\boldsymbol{k},\boldsymbol{k}')\right]\phi_{\boldsymbol{0}}(r_A), \tag{12}$$

where $f(\boldsymbol{k},\boldsymbol{k}')$ with $\boldsymbol{k}' \equiv k\hat{\boldsymbol{r}}_B$ defines the two-body scattering amplitude in the 0D-3D mixed dimensions:

$$f(\boldsymbol{k},\boldsymbol{k}') \equiv -\frac{1}{C}\frac{m_B}{m_{AB}}\int d\boldsymbol{r}' e^{-i\boldsymbol{k}'\cdot\boldsymbol{r}'}\phi^*_{\boldsymbol{0}}(r')\chi(\boldsymbol{r}'). \tag{13}$$

We note that χ has an implicit $\boldsymbol{k}$ dependence.

The unknown function χ can be determined by substituting the solution (8) into the Bethe-Peierls boundary condition (5). Defining the regular part of the Green's function $\mathcal{G}$ by

$$G_E(\boldsymbol{r}_A,\boldsymbol{r}_B;\boldsymbol{r}',\boldsymbol{r}')|_{\boldsymbol{r}_A,\boldsymbol{r}_B\to\boldsymbol{r}} \equiv -\frac{m_{AB}}{2\pi|\boldsymbol{r}_A-\boldsymbol{r}_B|}\delta(\boldsymbol{r}-\boldsymbol{r}')+\mathcal{G}(\boldsymbol{r};\boldsymbol{r}'), \tag{14}$$

we obtain

$$\frac{1}{\tilde{a}(\hat{E}_c)}\chi(\boldsymbol{r}) = Ce^{i\boldsymbol{k}\cdot\boldsymbol{r}}\phi_{\boldsymbol{0}}(r)+\frac{2\pi}{m_{AB}}\int d\boldsymbol{r}'\mathcal{G}(\boldsymbol{r};\boldsymbol{r}')\chi(\boldsymbol{r}'). \tag{15}$$

This integral equation determines χ/C, which in turn provides f from Eq. (13).

Because of the 3D rotational symmetries of the system, f, χ, and $\mathcal{G}$ can be decomposed into their partial-wave components:

$$f(\boldsymbol{k},\boldsymbol{k}') = \sum_{\ell=0}^{\infty}(2\ell+1)\,f_\ell(k)P_\ell(\hat{\boldsymbol{k}}\cdot\hat{\boldsymbol{k}}'), \tag{16}$$

$$\chi(\boldsymbol{r}) = \sum_{\ell=0}^{\infty}(2\ell+1)\,\chi_\ell(r)P_\ell(\hat{\boldsymbol{r}}\cdot\hat{\boldsymbol{k}}), \tag{17}$$

$$\mathcal{G}(\boldsymbol{r};\boldsymbol{r}') = \sum_{\ell=0}^{\infty}(2\ell+1)\,\mathcal{G}_\ell(r;r')P_\ell(\hat{\boldsymbol{r}}\cdot\hat{\boldsymbol{r}}'). \tag{18}$$

Equations (13) and (15) lead to the ℓth partial-wave scattering amplitude given by

$$f_\ell(k) = -\frac{1}{C}\frac{m_B}{m_{AB}}\int d\boldsymbol{r}'\,j_\ell(kr')\phi_{\boldsymbol{0}}^*(r')\chi_\ell(r') \tag{19}$$

with

$$\frac{1}{\tilde{a}(\hat{E}_c)}\chi_\ell(r) = Cj_\ell(kr)\phi_{\boldsymbol{0}}(r)+\frac{2\pi}{m_{AB}}\int d\boldsymbol{r}'\mathcal{G}_\ell(r;r')\chi_\ell(r'). \tag{20}$$

From the general argument based on the 3D rotational symmetries and unitarity [30], or from the explicit calculation that uses the Green's function in Eq. (9), we can show that f_ℓ has the usual low-energy expansion:

$$\lim_{k\to0} f_\ell(k) = -\frac{k^{2\ell}}{\frac{1}{a_{\rm eff}^{(\ell)}}-\frac{1}{2}r_{\rm eff}^{(\ell)}k^2+O(k^4)+ik^{2\ell+1}}, \tag{21}$$

where $a_{\rm eff}^{(\ell)}$ and $r_{\rm eff}^{(\ell)}$ are effective scattering "length" and "range" parameters in the ℓth partial-wave channel. Note that $a_{\rm eff}^{(\ell)}$ has the dimension of (length)$^{2\ell+1}$ and $r_{\rm eff}^{(\ell)}$ has (length)$^{1-2\ell}$.

Substituting the expansion of f_ℓ into Eq. (19), we can determine the low-energy scattering parameters. In particular, the effective scattering length $a_{\rm eff}^{(\ell)}$ is given by

$$a_{\rm eff}^{(\ell)} = \frac{1}{C}\frac{m_B}{m_{AB}}\frac{\sqrt{\pi}}{2^{\ell+1}\left(\ell+\frac{1}{2}\right)!}\int d\boldsymbol{r}'r'^\ell\phi_{\boldsymbol{0}}^*(r')\chi_\ell(r'), \tag{22}$$

with

$$\frac{1}{\tilde{a}(\hat{E}_c)}\chi_\ell(r) = C\frac{\sqrt{\pi}}{2^{\ell+1}\left(\ell+\frac{1}{2}\right)!}r^\ell\phi_{\boldsymbol{0}}(r) + \frac{2\pi}{m_{AB}}\int d\boldsymbol{r}'\mathcal{G}_\ell(r;r')\Big|_{k\to0}\chi_\ell(r'). \tag{23}$$

The ℓth partial-wave resonance in the 0D-3D mixed dimensions is defined by the divergence of $a_{\rm eff}^{(\ell)}\to\infty$, which occurs when

$$\frac{1}{\tilde{a}(\hat{E}_c)}\chi_\ell(r) = \frac{2\pi}{m_{AB}}\int d\boldsymbol{r}'\mathcal{G}_\ell(r;r')\Big|_{k\to0}\chi_\ell(r') \tag{24}$$

is satisfied.

B. Positions of resonances

We now solve the integral equation (24) numerically to determine the positions of ℓth partial-wave resonances. For the purpose of illustrating qualitative results, we shall set $r_{\rm 3D}=0$. For quantitative predictions in a specific atomic mixture, it is necessary but straightforward to include the effective range correction [27]. Some details of our method to solve the integral equation are shown in Appendix A.

Figure 2 shows the positions of the lowest five resonances in terms of $l_{\rm ho}/a_{\rm 3D}$ for $\ell=0,1,2,3$ partial-wave channels as functions of the mass ratio m_A/m_B. For completeness, we have included the result for the s-wave ($\ell=0$) resonance, which has been reported in Ref. [23]. As we have discussed in Sec. I, there exists a series of resonances in each partial-wave channel induced from the purely s-wave interaction in a free space. Indeed, the resonance positions are well described by the approximate formula $E_{AB}=\frac{3}{2}\hbar\omega$ by using Eq. (1) with $E_b=-\hbar^2/(2m_{AB}a_{\rm 3D}^2)$ in a wide range of the mass ratio $m_A/m_B\gtrsim1$. For such a mass ratio, as is evident from Eq. (1), d-wave (f-wave) resonances are nearly degenerate with s-wave (p-wave) resonances, and thus it could be difficult to distinguish them practically. We also note that the ℓth partial-wave resonance is $(2\ell+1)$-fold degenerate in a spherically symmetric potential. This degeneracy is lifted when the confinement potential is deformed, and therefore the one resonance at a given $l_{\rm ho}/a_{\rm 3D}$ splits into more resonances.

C. Confinement-induced molecules

On the $a_{\rm eff}^{(\ell)}>0$ side of every resonance, a shallow AB molecule is formed. In the vicinity of the resonance $a_{\rm eff}^{(\ell)}\gg l_{\rm ho}^{2\ell+1}$, its binding energy $\varepsilon_{AB}\equiv E-\frac{3}{2}\omega<0$ is determined by the pole of the scattering amplitude [Eq. (21)] with keeping the two dominant terms at $k\to0$:

$$\varepsilon_{AB} = \begin{cases} -\dfrac{1}{2m_Ba_{\rm eff}^{(\ell)2}} & \text{for} \quad \ell=0, \\ \dfrac{1}{m_Ba_{\rm eff}^{(\ell)}r_{\rm eff}^{(\ell)}} & \text{for} \quad \ell\geqslant1. \end{cases} \tag{25}$$

Away from the resonance, these universal formulas are no longer valid. The binding energy $\varepsilon_{AB}=-\kappa^2/(2m_B)$ has to be determined by solving the integral equation

$$\frac{1}{\tilde{a}(\hat{E}_c)}\chi_\ell^m(r) = \frac{2\pi}{m_{AB}}\int d\boldsymbol{r}'\mathcal{G}_\ell(r;r')\Big|_{k\to i\kappa}\chi_\ell^m(r'), \tag{26}$$

where χ_ℓ^m is a component of the spherical harmonics expansion of χ:

$$\chi(\boldsymbol{r}) = \sum_{\ell=0}^{\infty}\sum_{m=-\ell}^{\ell}\chi_\ell^m(r)Y_\ell^m(\hat{\boldsymbol{r}}). \tag{27}$$

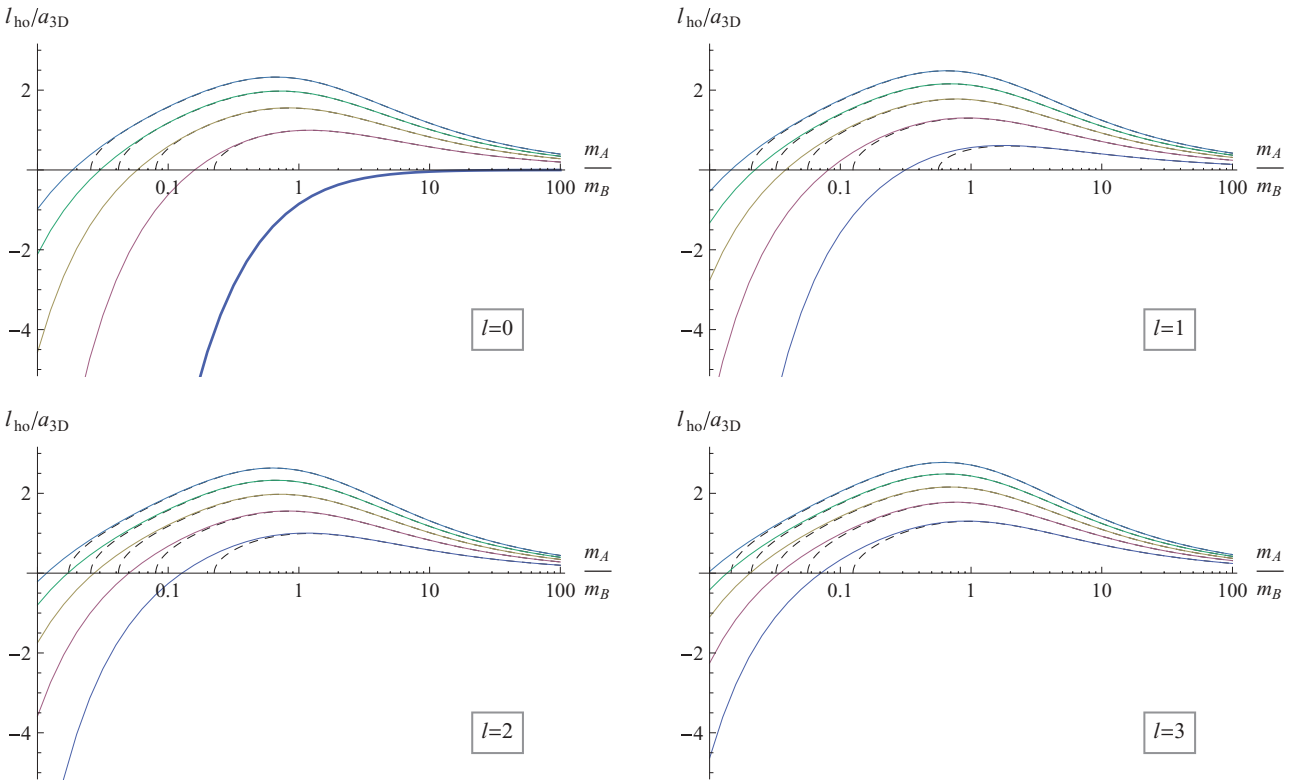

FIG. 2. (Color online) 0D-3D mixture: Positions of the lowest five resonances in terms of $l_{\rm ho}/a_{\rm 3D}$ for $\ell = 0$ (upper left), $\ell = 1$ (upper right), $\ell = 2$ (lower left), and $\ell = 3$ (lower right) channels as functions of the mass ratio m_A/m_B. The dashed curves are from the approximate formula $E_{AB} = \frac{3}{2}\hbar\omega$ by using Eq. (1) with $E_b = -\hbar^2/(2m_{AB}a_{\rm 3D}^2)$.

We note that the solution is independent of m, and therefore there are $2\ell + 1$ degenerate molecules for a spherically symmetric potential. This degeneracy is lifted when the confinement potential is deformed.

We now derive the asymptotic form of the molecular wave function in the vicinity of the ℓth partial-wave resonance where $l_{\rm ho} \ll \kappa^{-1} \ll |\boldsymbol{r}_B|$ is satisfied. From Eqs. (8) and (9) with the replacement $k \to i\kappa$, we find

$$\psi(\boldsymbol{r}_A,\boldsymbol{r}_B) \to -\sum_{m=-\ell}^{\ell} \frac{1}{2\ell+1}\frac{m_B}{m_{AB}}\frac{e^{-\kappa r_B}}{r_B^{\ell+1}}\phi_{\boldsymbol{0}}(r_A) \times Y_\ell^m(\hat{\boldsymbol{r}}_B)\int d\boldsymbol{r}' r'^{\ell}\phi_{\boldsymbol{0}}^*(r')\chi_\ell^m(r'). \quad (28)$$

The angular parts of asymptotic wave functions of three degenerate shallow p-wave molecules $\psi \sim Y_1^{0,\pm1}(\hat{\boldsymbol{r}}_B)$ are illustrated in Fig. 1.

D. Scattering parameters in the p-wave channel

The effective scattering length in the s-wave channel $a_{\rm eff} \equiv a_{\rm eff}^{(0)}$ has been computed in Ref. [23]. Here we focus on the p-wave ($\ell = 1$) channel and determine its two low-energy scattering parameters, namely, the effective scattering volume $v_{\rm eff} \equiv a_{\rm eff}^{(1)}$ and the effective momentum $k_{\rm eff} \equiv r_{\rm eff}^{(1)}$. The effective scattering volume can be computed by eliminating C from Eqs. (22) and (23) and solving the resulting integral equation numerically (see Appendix A for details). In Fig. 3, $v_{\rm eff}/l_{\rm ho}^3$ for $r_{\rm 3D} = 0$ is plotted as a function of $l_{\rm ho}/a_{\rm 3D}$ for three mass ratios $m_A/m_B = 6/40$, 1, and 40/6. We confirm the existence of a series of p-wave resonances ($v_{\rm eff} \to \infty$) induced from the purely s-wave interaction in a free space, while they become narrower for larger $l_{\rm ho}/a_{\rm 3D}$. We also find that the resonance is wider when a lighter atom is confined in lower dimensions.

Similarly, the effective momentum can be computed from Eq. (19), and $k_{\rm eff}l_{\rm ho}$ for $r_{\rm 3D} = 0$ is plotted in Fig. 3 as a function of $l_{\rm ho}/a_{\rm 3D}$ for the same three mass ratios. In the vicinity of the p-wave resonance $v_{\rm eff} \gg l_{\rm ho}^3$, $v_{\rm eff}$ and $k_{\rm eff}$ determine the binding energy of three degenerate shallow p-wave molecules via the universal formula (25). Both $v_{\rm eff}$ and $k_{\rm eff}$ are important to the low-energy effective theory of the p-wave resonance discussed below.

E. Low-energy effective theory

The low-energy effective theory of the p-wave resonance in the 0D-3D mixed dimensions is provided by the action

$$\begin{aligned} S = &\int dt\,\Psi_A^\dagger(t)\,(i\partial_t)\,\Psi_A(t) \\ &+ \int dt d\boldsymbol{r}\,\Psi_B^\dagger(t,\boldsymbol{r})\left(i\partial_t + \frac{\boldsymbol{\nabla}_{\boldsymbol{r}}^2}{2m_B}\right)\Psi_B(t,\boldsymbol{r}) \\ &+ \int dt\,\Phi_j^\dagger(t)\,(i\partial_t + \varepsilon_0)\,\Phi_j(t) \\ &+ g_0\int dt[\Psi_A^\dagger(t)\nabla_j\Psi_B^\dagger(t,\boldsymbol{0})\Phi_j(t) \\ &+ \Phi_j^\dagger(t)\nabla_j\Psi_B(t,\boldsymbol{0})\Psi_A(t)], \end{aligned} \quad (29)$$

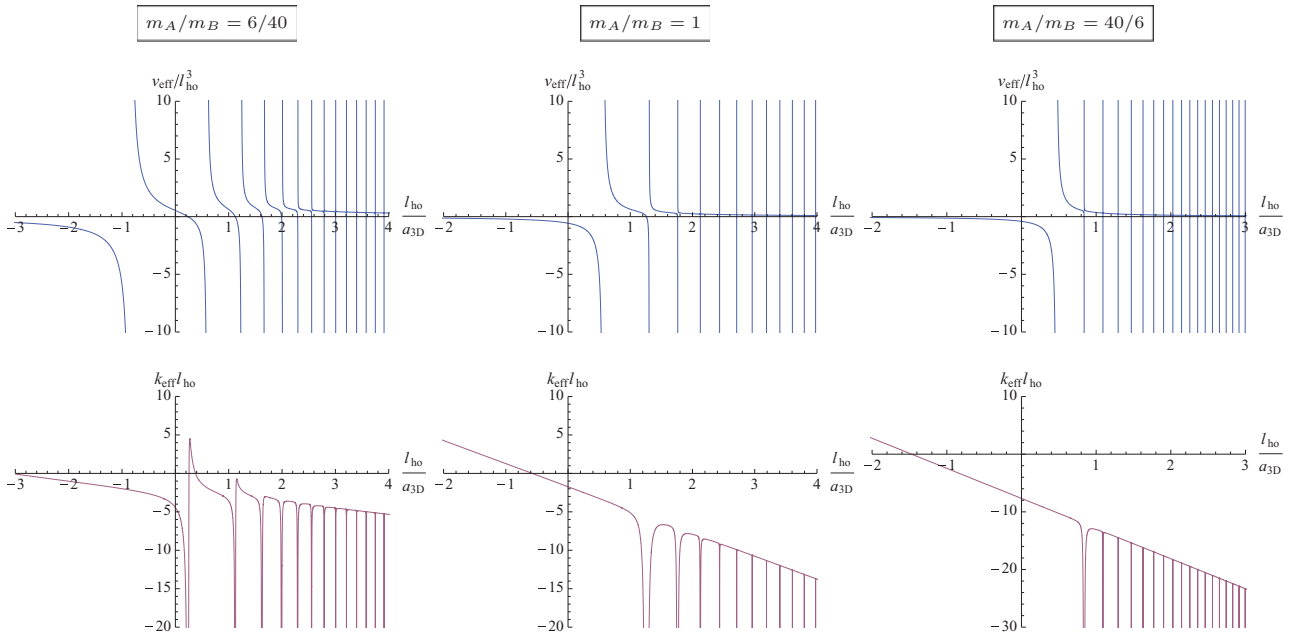

FIG. 3. (Color online) 0D-3D mixture: p-wave effective scattering volume $v_{\rm eff}/l_{\rm ho}^3$ (upper figures) and effective momentum $k_{\rm eff} l_{\rm ho}$ (lower figures) as functions of $l_{\rm ho}/a_{\rm 3D}$ for mass ratios $m_A/m_B = 6/40$ (left), 1 (middle), and 40/6 (right).

where the summation over $j = x, y, z$ is implicitly understood. Ψ_A and Ψ_B fields represent the A and B atoms in 0D and 3D, respectively. The interaction between A and B atoms is described through their coupling with three p-wave molecular fields Φ_j. g_0 is their coupling strength and ε_0 is the detuning from the resonance. These cutoff (Λ)-dependent bare parameters can be related to the effective scattering volume $v_{\rm eff}$ and effective momentum $k_{\rm eff}$ by matching the two-body scattering amplitude from the action (29) with that shown in Eqs. (16) and (21).

The standard diagrammatic calculation leads to the following scattering amplitude with collision energy $\varepsilon = k^2/(2m_B)$:

$$i\mathcal{A}(k) = -\frac{i\boldsymbol{k}\cdot\boldsymbol{k}'}{\frac{k^2/(2m_B)+\varepsilon_0}{g_0^2} + \frac{m_B}{3\pi^2}\left(\frac{\Lambda^3}{3} + \Lambda k^2 + \frac{\pi}{2} i k^3\right)}. \quad (30)$$

By defining

$$\frac{\varepsilon_0}{g_0^2} + \frac{m_B}{3\pi^2}\frac{\Lambda^3}{3} \equiv \frac{m_B}{6\pi}\frac{1}{v_{\rm eff}} \quad (31)$$

and

$$\frac{1}{2m_B g_0^2} + \frac{m_B}{3\pi^2}\Lambda \equiv -\frac{m_B}{6\pi}\frac{k_{\rm eff}}{2}, \quad (32)$$

we reproduce the scattering amplitude (21) in the p-wave ($\ell = 1$) channel up to a kinematical factor:

$$\mathcal{A}(k) = -\frac{2\pi}{m_B}\frac{3\boldsymbol{k}\cdot\boldsymbol{k}'}{\frac{1}{v_{\rm eff}} - \frac{k_{\rm eff}}{2}k^2 + ik^3}. \quad (33)$$

This low-energy effective theory can be generalized easily to the case with more than one lattice site where B atoms are confined and could be used to investigate the many-body physics across the p-wave resonance as in the 3D case [31]. We note that an effective field theory of the p-wave resonance in 3D has been developed in connection with the α-n scattering [32,33].

F. Weak-coupling limit

When $a_{\rm 3D} < 0$ and $|a_{\rm 3D}| \ll l_{\rm ho}$, the confinement-induced resonances can be understood in a different way, as is discussed in Refs. [23] and [34]. To the leading order in the weak-coupling expansion $a_{\rm 3D}/l_{\rm ho} \to -0$, an A atom occupies the ground state in a 3D harmonic potential and creates a mean-field attractive potential felt by a B atom. Therefore, the scattering of the B atom by the confined A atom is described by

$$\left[-\frac{\nabla_{\boldsymbol{r}_B}^2}{2m_B} + \frac{2\pi a_{\rm 3D}}{m_{AB}}|\phi_{\boldsymbol{0}}(r_B)|^2\right]\psi(\boldsymbol{r}_B) = \frac{k^2}{2m_B}\psi(\boldsymbol{r}_B), \quad (34)$$

where $|\phi_{\boldsymbol{0}}(r)|^2 = e^{-r^2/l_{\rm ho}^2}/(\sqrt{\pi} l_{\rm ho})^3$. This Schrödinger equation, which is valid in the weak-coupling limit, is equivalent to the integral equation (15), where only the $\boldsymbol{n} = \boldsymbol{0}$ term is kept in the Green's function (9) and $\chi(\boldsymbol{r})$ is identified as $a_{\rm 3D}\phi_{\boldsymbol{0}}(r)\psi(\boldsymbol{r})$.

By matching the solution of Eq. (34) with the asymptotic form (12), we can determine the scattering amplitude and low-energy scattering parameters in the weak-coupling limit $|a_{\rm 3D}| \ll l_{\rm ho}$. In particular, the resonance occurs when a new bound state appears. This is possible even in the weak-coupling limit because the attractive potential becomes strong compared to the kinetic term by decreasing the mass ratio down to $m_A/m_B \ll 1$. We find that the resonances are achieved at the critical values of $(m_B/m_{AB})(a_{\rm 3D}/l_{\rm ho}) = -1.19, -7.89, -20.2, \ldots$ in the $\ell = 0$ channel [23,34], $(m_B/m_{AB})(a_{\rm 3D}/l_{\rm ho}) = -5.36, -15.5, -31.2, \ldots$ in the $\ell = 1$ channel, $(m_B/m_{AB})(a_{\rm 3D}/l_{\rm ho}) = -11.9, -25.6, -44.6, \ldots$ in the $\ell = 2$ channel, and $(m_B/m_{AB})(a_{\rm 3D}/l_{\rm ho}) = -20.9, -37.9, -60.4, \ldots$ in the $\ell = 3$ channel.

III. 1D-3D MIXED DIMENSIONS

A. Scattering theory [35]

The scattering of a quasi-1D A atom with a B atom in 3D is described by a Schrödinger equation,

$$\left(-\frac{\nabla_{\boldsymbol{\rho}_A}^2}{2m_A}+\frac{1}{2}m_A\omega^2\boldsymbol{\rho}_A^2-\frac{\nabla_{\boldsymbol{\rho}_B}^2}{2m_B}-\frac{\nabla_{z_{AB}}^2}{2m_{AB}}\right)\psi(\boldsymbol{\rho}_A,\boldsymbol{\rho}_B,z_{AB}) = E\psi(\boldsymbol{\rho}_A,\boldsymbol{\rho}_B,z_{AB}) \tag{35}$$

for $\sqrt{(\boldsymbol{\rho}_A-\boldsymbol{\rho}_B)^2+z_{AB}^2}>0$, where $\boldsymbol{\rho}\equiv(x,y)$, $z_{AB}\equiv z_A-z_B$, and the center-of-mass motion in the z direction is eliminated. The short-range interspecies interaction is implemented by the generalized Bethe-Peierls boundary condition [28,29]:

$$\psi(\boldsymbol{\rho}_A,\boldsymbol{\rho}_B,z_{AB})|_{\boldsymbol{\rho}_A,\boldsymbol{\rho}_B\to\boldsymbol{\rho};z_{AB}\to 0} \to\left[\frac{1}{\tilde{a}(\hat{E}_c)}-\frac{1}{\sqrt{(\boldsymbol{\rho}_A-\boldsymbol{\rho}_B)^2+z_{AB}^2}}\right]\chi(\boldsymbol{\rho}). \tag{36}$$

The collision energy operator $\hat{E}_c$ in Eq. (6) in the present case is given by

$$\hat{E}_c = E-\left(-\frac{\nabla_{\boldsymbol{\rho}}^2}{2M}+\frac{1}{2}m_A\omega^2\boldsymbol{\rho}^2\right). \tag{37}$$

The solution to the Schrödinger equation (35) can be written as

$$\psi(\boldsymbol{\rho}_A,\boldsymbol{\rho}_B,z_{AB})=\psi_0(\boldsymbol{\rho}_A,\boldsymbol{\rho}_B,z_{AB}) +\frac{2\pi}{m_{AB}}\int d\boldsymbol{\rho}' G_E(\boldsymbol{\rho}_A,\boldsymbol{\rho}_B,z_{AB};\boldsymbol{\rho}',\boldsymbol{\rho}',0)\chi(\boldsymbol{\rho}'), \tag{38}$$

where ψ_0 is a solution in the noninteracting limit and G_E is the retarded Green's function for the noninteracting Hamiltonian:

$$\begin{aligned} &G_E(\boldsymbol{\rho}_A,\boldsymbol{\rho}_B,z_{AB};\boldsymbol{\rho}'_A,\boldsymbol{\rho}'_B,z'_{AB})\\ &\equiv\langle\boldsymbol{\rho}_A,\boldsymbol{\rho}_B,z_{AB}|\frac{1}{E-H_0+i0^+}|\boldsymbol{\rho}'_A,\boldsymbol{\rho}'_B,z'_{AB}\rangle\\ &=-\frac{\sqrt{m_Bm_{AB}}}{2\pi}\sum_{\boldsymbol{n}}\phi_{\boldsymbol{n}}(\boldsymbol{\rho}_A)\phi_{\boldsymbol{n}}^*(\boldsymbol{\rho}'_A)\\ &\times\frac{e^{-\sqrt{2m_B}\sqrt{(n_x+n_y+1)\omega-E-i0^+}|\tilde{\boldsymbol{r}}_B-\tilde{\boldsymbol{r}}'_B|}}{|\tilde{\boldsymbol{r}}_B-\tilde{\boldsymbol{r}}'_B|}. \end{aligned} \tag{39}$$

Here $\phi_{\boldsymbol{n}}$ with quantum numbers $\boldsymbol{n}=(n_x,n_y)$ is the normalized wave function of an A atom in the 2D harmonic potential, and $\tilde{\boldsymbol{r}}_B\equiv(\boldsymbol{\rho}_B,-\sqrt{\frac{m_{AB}}{m_B}}z_{AB})$ are coordinates of the B atom relative to the confined A atom. The anisotropic factor is such because separations in the x and y directions are associated with m_B while a separation in the z direction is associated with m_{AB} [see the last two terms in Eq. (35)].

We now consider the low-energy scattering in which

$$E-\omega\equiv\frac{k^2}{2m_B}\ll\omega \tag{40}$$

is satisfied, and then ψ_0 becomes

$$\psi_0(\boldsymbol{\rho}_A,\boldsymbol{\rho}_B,z_{AB})=Ce^{i\boldsymbol{k}\cdot\tilde{\boldsymbol{r}}_B}\phi_{\boldsymbol{0}}(\rho_A), \tag{41}$$

which represents the A atom in the ground state of the 2D harmonic potential and the plane wave of B atom with the wave vector $\boldsymbol{k}$. The asymptotic form of the wave function at a large distance $|\tilde{\boldsymbol{r}}_B|\gg l_{\rm ho}$ is given by

$$\psi(\boldsymbol{\rho}_A,\boldsymbol{\rho}_B,z_{AB})\to C\left[e^{i\boldsymbol{k}\cdot\tilde{\boldsymbol{r}}_B}+\frac{e^{ik\tilde{r}_B}}{\tilde{r}_B}f(\boldsymbol{k}_\perp,\boldsymbol{k}'_\perp)\right]\phi_{\boldsymbol{0}}(\rho_A), \tag{42}$$

where $f(\boldsymbol{k}_\perp,\boldsymbol{k}'_\perp)$ with $\boldsymbol{k}'\equiv k\hat{\tilde{\boldsymbol{r}}}_B$ defines the two-body scattering amplitude in the 1D-3D mixed dimensions:

$$f(\boldsymbol{k}_\perp,\boldsymbol{k}'_\perp)\equiv-\frac{1}{C}\sqrt{\frac{m_B}{m_{AB}}}\int d\boldsymbol{\rho}' e^{-i\boldsymbol{k}'_\perp\cdot\boldsymbol{\rho}'}\phi_{\boldsymbol{0}}^*(\rho')\chi(\boldsymbol{\rho}'). \tag{43}$$

We note that χ has an implicit $\boldsymbol{k}_\perp\equiv(k_x,k_y)$ dependence and both χ and f depend on k through the Green's function (39).

The unknown function χ can be determined by substituting the solution (38) into the Bethe-Peierls boundary condition (36). Defining the regular part of the Green's function $\mathcal{G}$ by

$$\begin{aligned} &G_E(\boldsymbol{\rho}_A,\boldsymbol{\rho}_B,z_{AB};\boldsymbol{\rho}',\boldsymbol{\rho}',0)|_{\boldsymbol{\rho}_A,\boldsymbol{\rho}_B\to\boldsymbol{\rho};z_{AB}\to 0}\\ &\equiv-\frac{m_{AB}}{2\pi\sqrt{(\boldsymbol{\rho}_A-\boldsymbol{\rho}_B)^2+z_{AB}^2}}\delta(\boldsymbol{\rho}-\boldsymbol{\rho}')+\mathcal{G}(\boldsymbol{\rho};\boldsymbol{\rho}'), \end{aligned} \tag{44}$$

we obtain

$$\frac{1}{\tilde{a}(\hat{E}_c)}\chi(\boldsymbol{\rho})=Ce^{i\boldsymbol{k}_\perp\cdot\boldsymbol{\rho}}\phi_{\boldsymbol{0}}(\rho)+\frac{2\pi}{m_{AB}}\int d\boldsymbol{\rho}'\mathcal{G}(\boldsymbol{\rho};\boldsymbol{\rho}')\chi(\boldsymbol{\rho}'). \tag{45}$$

This integral equation determines χ/C, which in turn provides f from Eq. (43).

Because the system has a rotational symmetry in the xy plane, f, χ, and $\mathcal{G}$ can be decomposed into their partial-wave components:

$$f(\boldsymbol{k}_\perp,\boldsymbol{k}'_\perp)=\sum_{m=-\infty}^{\infty}f_m(k_\perp,k'_\perp)e^{im\arccos\hat{\boldsymbol{k}}_\perp\cdot\hat{\boldsymbol{k}}'_\perp}, \tag{46}$$

$$\chi(\boldsymbol{\rho})=\sum_{m=-\infty}^{\infty}\chi_m(\rho)e^{im\arccos\hat{\boldsymbol{\rho}}\cdot\hat{\boldsymbol{k}}_\perp}, \tag{47}$$

$$\mathcal{G}(\boldsymbol{\rho};\boldsymbol{\rho}')=\sum_{m=-\infty}^{\infty}\mathcal{G}_m(\rho;\rho')e^{im\arccos\hat{\boldsymbol{\rho}}\cdot\hat{\boldsymbol{\rho}}'}. \tag{48}$$

Because m and $-m$ are degenerate, we assume $m\geqslant 0$ in this section without loss of generality. Equations (43) and (45) lead to the mth partial-wave scattering amplitude given by

$$f_m(k_\perp,k'_\perp)=-\frac{1}{C}\sqrt{\frac{m_B}{m_{AB}}}\int d\boldsymbol{\rho}' J_m(k_\perp\rho')\phi_{\boldsymbol{0}}^*(\rho')\chi_m(\rho'), \tag{49}$$

with

$$\frac{1}{\tilde{a}(\hat{E}_c)}\chi_m(\rho)=CJ_m(k_\perp\rho)\phi_{\boldsymbol{0}}(\rho) +\frac{2\pi}{m_{AB}}\int d\boldsymbol{\rho}'\mathcal{G}_m(\rho;\rho')\chi_m(\rho'). \tag{50}$$

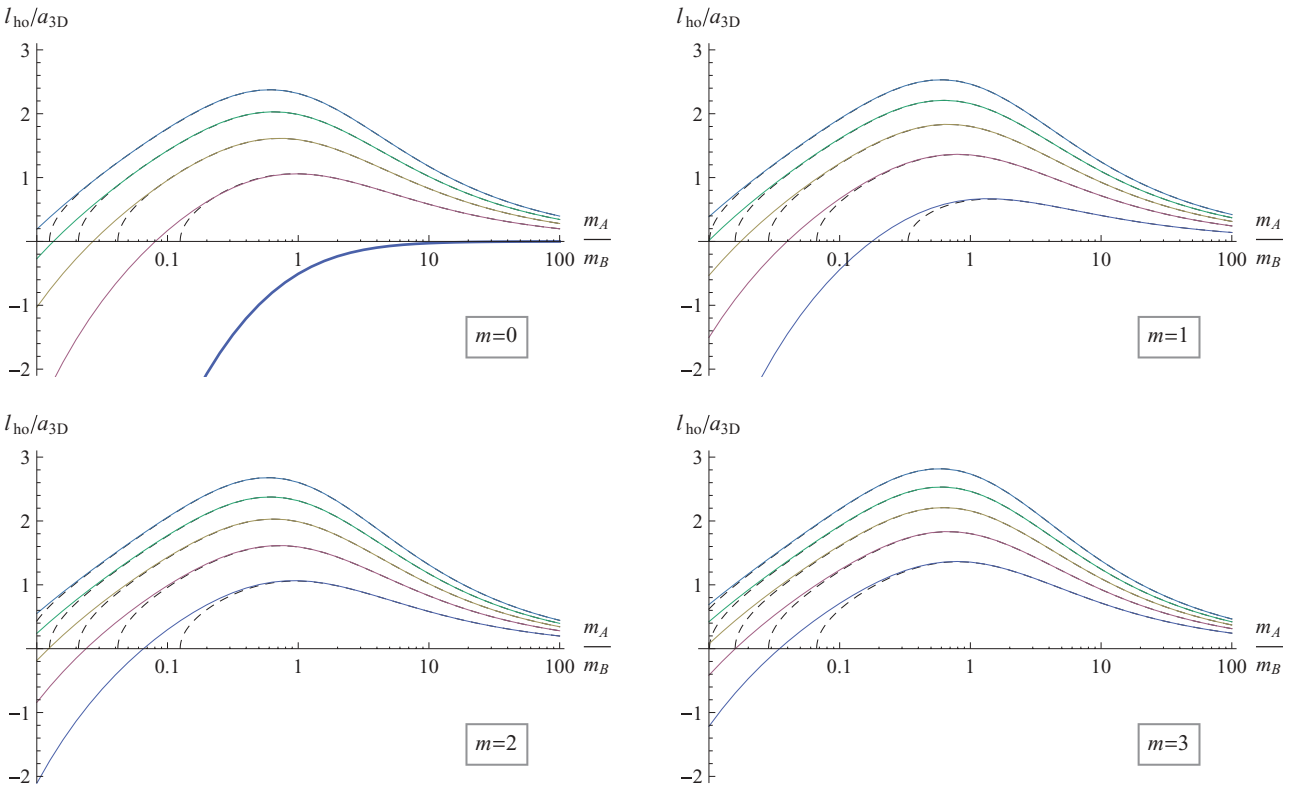

FIG. 4. (Color online) 1D-3D mixture: Positions of the lowest five resonances in terms of l_{ho}/a_{3D} for $m = 0$ (upper left), $m = 1$ (upper right), $m = 2$ (lower left), and $m = 3$ (lower right) channels as functions of the mass ratio m_A/m_B. The dashed curves are from the approximate formula $E_{AB} = \hbar\omega$ by using Eq. (2) with $E_b = -\hbar^2/(2m_{AB}a_{3D}^2)$.

From the explicit calculation that uses the Green's function in Eq. (39), we can show that f_m has the following low-energy expansion:

$$\lim_{k\to 0} f_m(k) = -\frac{\frac{(2m+1)!}{(2^m m!)^2}k_\perp^m k_\perp'^m}{\frac{1}{a_{\rm eff}^{(m)}} - \frac{1}{2}r_{\rm eff}^{(m)}k^2 + O(k^4) + ik^{2m+1}[1+O(k^2)]} + O(k_\perp^{m+2}k_\perp'^m, k_\perp^m k_\perp'^{m+2}), \quad (51)$$

where $a_{\rm eff}^{(m)}$ and $r_{\rm eff}^{(m)}$ are effective scattering "length" and "range" parameters in the mth partial-wave channel. Note that $a_{\rm eff}^{(m)}$ has the dimension of (length)$^{2m+1}$ and $r_{\rm eff}^{(m)}$ has (length)$^{1-2m}$. This unusual form of the low-energy expansion is owing to the lack of full 3D rotational symmetries.

Substituting the expansion of f_m into Eq. (49), we can determine the low-energy scattering parameters. In particular, the effective scattering length $a_{\rm eff}^{(m)}$ is given by

$$\frac{(2m+1)!}{(2^m m!)^2}a_{\rm eff}^{(m)} = \frac{1}{C}\sqrt{\frac{m_B}{m_{AB}}}\frac{1}{2^m m!}\int d\boldsymbol{\rho}'\rho'^m\phi_{\mathbf{0}}^*(\rho')\chi_m(\rho'), \quad (52)$$

with

$$\frac{1}{\tilde{a}(\hat{E}_c)}\chi_m(\rho) = C\frac{1}{2^m m!}\rho^m\phi_{\mathbf{0}}(\rho) + \frac{2\pi}{m_{AB}}\int d\boldsymbol{\rho}'\mathcal{G}_m(\rho;\rho')\Big|_{k\to 0}\chi_m(\rho'). \quad (53)$$

The mth partial-wave resonance in the 1D-3D mixed dimensions is defined by the divergence of $a_{\rm eff}^{(m)} \to \infty$, which occurs when

$$\frac{1}{\tilde{a}(\hat{E}_c)}\chi_m(\rho) = \frac{2\pi}{m_{AB}}\int d\boldsymbol{\rho}'\mathcal{G}_m(\rho;\rho')\Big|_{k\to 0}\chi_m(\rho') \quad (54)$$

is satisfied.

B. Positions of resonances

We now solve the integral equation (54) numerically to determine the positions of $|m|$th partial-wave resonances. For the purpose of illustrating qualitative results, we shall set $r_{3D} = 0$. For quantitative predictions in a specific atomic mixture, it is necessary but straightforward to include the effective range correction [27]. Some details of our method to solve the integral equation are shown in Appendix B.

Figure 4 shows the positions of the lowest five resonances in terms of l_{ho}/a_{3D} for $m = 0,1,2,3$ partial-wave channels as functions of the mass ratio m_A/m_B. For completeness, we have included the result for the s-wave ($m = 0$) resonance, which has been reported in Ref. [24]. As we have discussed in Sec. I, there exists a series of resonances in each partial-wave channel induced from the purely s-wave interaction in a free space. Indeed, the resonance positions are well described by the approximate formula $E_{AB} = \hbar\omega$ by using Eq. (2) with $E_b = -\hbar^2/(2m_{AB}a_{3D}^2)$ in a wide range of the mass ratio $m_A/m_B \gtrsim 1$. For such a mass ratio, as is evident from Eq. (2), d-wave (f-wave) resonances are nearly degenerate

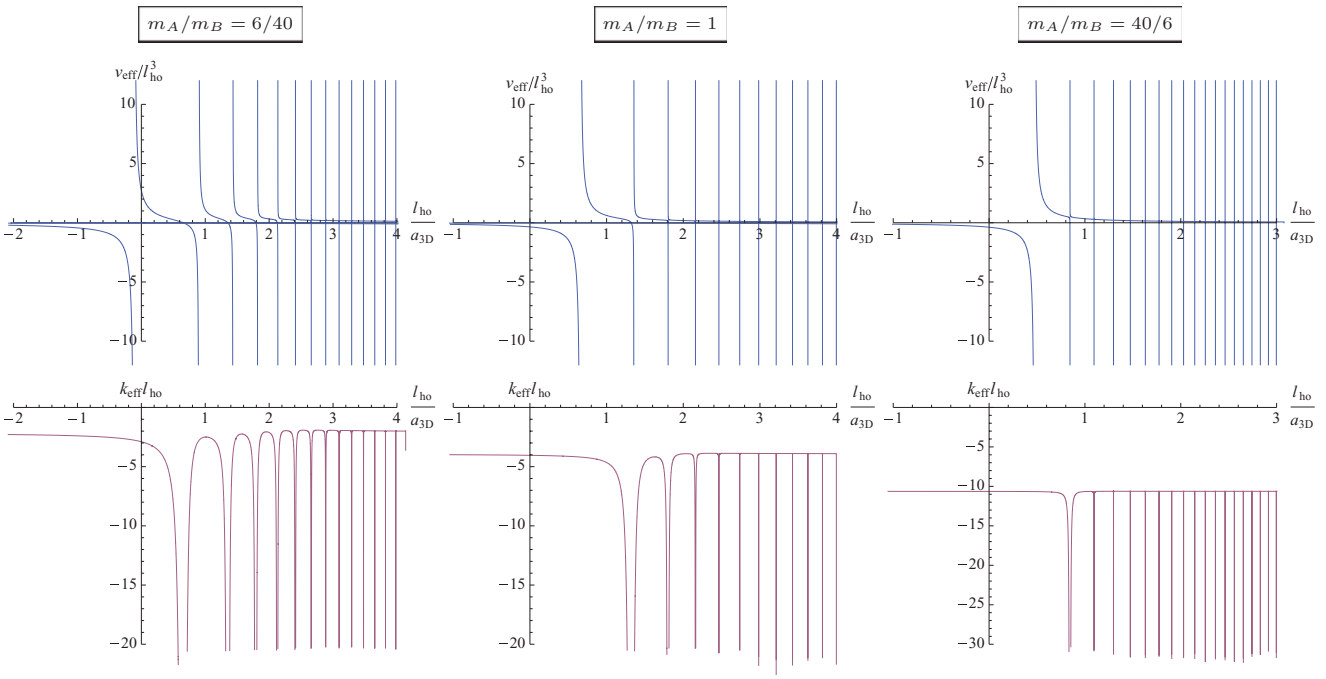

FIG. 5. (Color online) 1D-3D mixture: p-wave effective scattering volume $v_{\rm eff}/l_{\rm ho}^3$ (upper figures) and effective momentum $k_{\rm eff} l_{\rm ho}$ (lower figures) as functions of $l_{\rm ho}/a_{\rm 3D}$ for mass ratios $m_A/m_B = 6/40$ (left), 1 (middle), and 40/6 (right).

with s-wave (p-wave) resonances, and thus it could be difficult to distinguish them practically. We also note that the $|m|$th partial-wave resonance for $|m| \geqslant 1$ is twofold degenerate in a circularly symmetric potential. This degeneracy is lifted when the confinement potential is deformed, and therefore the one resonance at a given $l_{\rm ho}/a_{\rm 3D}$ splits into two resonances.

C. Confinement-induced molecules

On the $a_{\rm eff}^{(m)} > 0$ side of every resonance, a shallow AB molecule is formed. In the vicinity of the resonance $a_{\rm eff}^{(m)} \gg l_{\rm ho}^{2|m|+1}$, its binding energy $\varepsilon_{AB} \equiv E - \omega < 0$ is determined by the pole of the scattering amplitude [Eq. (51)] with keeping the two dominant terms at $k \to 0$:

$$\varepsilon_{AB} = \begin{cases} -\dfrac{1}{2m_B a_{\rm eff}^{(m)2}} & \text{for} \quad m = 0, \\ \dfrac{1}{m_B a_{\rm eff}^{(m)} r_{\rm eff}^{(m)}} & \text{for} \quad |m| \geqslant 1. \end{cases} \tag{55}$$

Away from the resonance, these universal formulas are no longer valid. The binding energy $\varepsilon_{AB} = -\kappa^2/(2m_B)$ has to be determined by solving the integral equation

$$\frac{1}{\tilde{a}(\hat{E}_c)} \chi_m(\rho) = \frac{2\pi}{m_{AB}} \int d\boldsymbol{\rho}' \mathcal{G}_m(\rho; \rho') \Big|_{k \to i\kappa} \chi_m(\rho'). \tag{56}$$

We note that the solution for $|m| \geqslant 1$ is independent of the sign of m, and therefore there are two degenerate molecules for a circularly symmetric potential. This degeneracy is lifted when the confinement potential is deformed.

We now derive the asymptotic form of the molecular wave function in the vicinity of the $|m|$th partial-wave resonance where $l_{\rm ho} \ll \kappa^{-1} \ll |\tilde{\boldsymbol{r}}_B|$ is satisfied. From Eqs. (38) and (39) with the replacement $k \to i\kappa$, we find

$$\begin{aligned} &\psi(\boldsymbol{\rho}_A, \boldsymbol{\rho}_B, z_{AB}) \\ &\to -\sum_{m=\pm|m|} \sum_{\ell=|m|}^{\infty} \sqrt{\frac{4\pi}{2\ell+1} \frac{(\ell-m)!}{(\ell+m)!}} P_\ell^m(0) \sqrt{\frac{m_B}{m_{AB}}} \\ &\quad \times \frac{e^{-\kappa \tilde{r}_B}}{\tilde{r}_B^{\ell+1}} \phi_{\mathbf{0}}(\rho_A) Y_\ell^m(\hat{\tilde{\boldsymbol{r}}}_B) \int d\boldsymbol{\rho}' \rho'^{\ell} \phi_{\mathbf{0}}^*(\rho') \chi_m(\rho'). \end{aligned} \tag{57}$$

One can see that different spherical harmonics $\sim Y_\ell^m$ with the same magnetic quantum number m contribute owing to the lack of full 3D rotational symmetries. The s-wave nature of the free-space interaction ensures that only $\ell = |m|, |m|+2, |m|+4, \ldots$ contribute so that the wave function is an even function of z_{AB}. The asymptotic behavior at a large separation $|\tilde{\boldsymbol{r}}_B| \to \infty$ is dominated by the $\ell = |m|$ component. The angular parts of asymptotic wave functions of two degenerate shallow p-wave molecules $\psi \sim Y_1^{\pm 1}(\hat{\tilde{\boldsymbol{r}}}_B)$ are illustrated in Fig. 1.

D. Scattering parameters in the p-wave channel

The effective scattering length in the s-wave channel $a_{\rm eff} \equiv a_{\rm eff}^{(0)}$ has been computed in Ref. [24]. Here we focus on the p-wave ($|m| = 1$) channel and determine its two low-energy scattering parameters, namely, the effective scattering volume $v_{\rm eff} \equiv a_{\rm eff}^{(1)}$ and the effective momentum $k_{\rm eff} \equiv r_{\rm eff}^{(1)}$. The effective scattering volume can be computed by eliminating C from Eqs. (52) and (53) and solving the resulting integral equation numerically (see Appendix B for details). In Fig. 5, $v_{\rm eff}/l_{\rm ho}^3$ for $r_{\rm 3D} = 0$ is plotted as a function of $l_{\rm ho}/a_{\rm 3D}$ for three mass ratios $m_A/m_B = 6/40$, 1, and 40/6. We confirm

the existence of a series of p-wave resonances ($v_{\rm eff} \to \infty$) induced from the purely s-wave interaction in a free space, while they become narrower for larger $l_{\rm ho}/a_{\rm 3D}$. We also find that the resonance is wider when a lighter atom is confined in lower dimensions.

Similarly, the effective momentum can be computed from Eq. (49), and $k_{\rm eff} l_{\rm ho}$ for $r_{\rm 3D} = 0$ is plotted in Fig. 5 as a function of $l_{\rm ho}/a_{\rm 3D}$ for the same three mass ratios. In the vicinity of the p-wave resonance $v_{\rm eff} \gg l_{\rm ho}^3$, $v_{\rm eff}$ and $k_{\rm eff}$ determine the binding energy of two degenerate shallow p-wave molecules via the universal formula (55). Both $v_{\rm eff}$ and $k_{\rm eff}$ are important to the low-energy effective theory of the p-wave resonance discussed below.

E. Low-energy effective theory

The low-energy effective theory of the p-wave resonance in the 1D-3D mixed dimensions is provided by the action

$$\begin{aligned} S = & \int dtdz \Psi_A^\dagger(t,z) \left(i\partial_t + \frac{\nabla_z^2}{2m_A} \right) \Psi_A(t,z) \\ & + \int dtdzd\boldsymbol{\rho} \Psi_B^\dagger(t,z,\boldsymbol{\rho}) \left(i\partial_t + \frac{\nabla_z^2 + \nabla_{\boldsymbol{\rho}}^2}{2m_B} \right) \Psi_B(t,z,\boldsymbol{\rho}) \\ & + \int dtdz \Phi_j^\dagger(t,z) \left(i\partial_t + \frac{\nabla_z^2}{2M} + \varepsilon_0 \right) \Phi_j(t,z) \\ & + g_0 \int dtdz [\Psi_A^\dagger(t,z) \nabla_j \Psi_B^\dagger(t,z,\mathbf{0}) \Phi_j(t,z) \\ & + \Phi_j^\dagger(t,z) \nabla_j \Psi_B(t,z,\mathbf{0}) \Psi_A(t,z)], \end{aligned} \tag{58}$$

where the summation over $j = x,y$ is implicitly understood. Ψ_A and Ψ_B fields represent the A and B atoms in 1D and 3D, respectively. The interaction between A and B atoms is described through their coupling with two p-wave molecular fields Φ_j. g_0 is their coupling strength and ε_0 is the detuning from the resonance. These cutoff (Λ)-dependent bare parameters can be related to the effective scattering volume $v_{\rm eff}$ and effective momentum $k_{\rm eff}$ by matching the two-body scattering amplitude from the action (58) with that shown in Eqs. (46) and (51).

The standard diagrammatic calculation leads to the following scattering amplitude with collision energy $\varepsilon = k^2/(2m_B)$:

$$i\mathcal{A}(k) = -\frac{i\boldsymbol{k}_\perp \cdot \boldsymbol{k}'_\perp}{\frac{k^2/(2m_B)+\varepsilon_0}{g_0^2} + \frac{\sqrt{m_B m_{AB}}}{3\pi^2}\left(\frac{\Lambda^3}{3} + \Lambda k^2 + \frac{\pi}{2} i k^3\right)}. \tag{59}$$

By defining

$$\frac{\varepsilon_0}{g_0^2} + \frac{\sqrt{m_B m_{AB}}}{3\pi^2}\frac{\Lambda^3}{3} \equiv \frac{\sqrt{m_B m_{AB}}}{6\pi}\frac{1}{v_{\rm eff}} \tag{60}$$

and

$$\frac{1}{2m_B g_0^2} + \frac{\sqrt{m_B m_{AB}}}{3\pi^2}\Lambda \equiv -\frac{\sqrt{m_B m_{AB}}}{6\pi}\frac{k_{\rm eff}}{2}, \tag{61}$$

we reproduce the scattering amplitude (51) in the p-wave ($|m| = 1$) channel up to a kinematical factor:

$$\mathcal{A}(k) = -\frac{2\pi}{\sqrt{m_B m_{AB}}} \frac{3\boldsymbol{k}_\perp \cdot \boldsymbol{k}'_\perp}{\frac{1}{v_{\rm eff}} - \frac{k_{\rm eff}}{2}k^2 + ik^3}. \tag{62}$$

This low-energy effective theory can be generalized easily to the case with more than one tube where B atoms are confined and could be used to investigate the many-body physics across the p-wave resonance as in the 3D case [31]. We note that the low-energy effective theory of the s-wave resonance in the 1D-3D mixed dimensions has been derived and used to study three-body problems in Ref. [36].

F. Weak-coupling limit

When $a_{\rm 3D} < 0$ and $|a_{\rm 3D}| \ll l_{\rm ho}$, the confinement-induced resonances can be understood in a different way. To the leading order in the weak-coupling expansion $a_{\rm 3D}/l_{\rm ho} \to -0$, an A atom occupies the ground state in a 2D harmonic potential and creates a mean-field attractive potential felt by a B atom. Therefore, the scattering of the B atom by the confined A atom is described by

$$\begin{aligned} & \left[-\frac{\nabla_{\boldsymbol{\rho}_B}^2}{2m_B} - \frac{\nabla_{z_{AB}}^2}{2m_{AB}} + \frac{2\pi a_{\rm 3D}}{m_{AB}} |\phi_{\mathbf{0}}(\rho_B)|^2 \delta(z_{AB}) \right] \psi(\boldsymbol{\rho}_B, z_{AB}) \\ & = \frac{k^2}{2m_B} \psi(\boldsymbol{\rho}_B, z_{AB}), \end{aligned} \tag{63}$$

where $|\phi_{\mathbf{0}}(\rho)|^2 = e^{-\rho^2/l_{\rm ho}^2}/(\sqrt{\pi} l_{\rm ho})^2$. This Schrödinger equation, which is valid in the weak-coupling limit, is equivalent to the integral equation (45), where only the $\boldsymbol{n} = \mathbf{0}$ term is kept in the Green's function (39) and $\chi(\boldsymbol{\rho})$ is identified as $a_{\rm 3D}\phi_{\mathbf{0}}(\rho)\psi(\boldsymbol{\rho},0)$.

By matching the solution of Eq. (63) with the asymptotic form (42), we can determine the scattering amplitude and low-energy scattering parameters in the weak-coupling limit $|a_{\rm 3D}| \ll l_{\rm ho}$. In particular, the resonance occurs when a new bound state appears. This is possible even in the weak-coupling limit because the attractive potential becomes strong compared to the kinetic term by decreasing the mass ratio down to $m_A/m_B \ll 1$. We find that the resonances are achieved at the critical values of $\sqrt{m_B/m_{AB}}(a_{\rm 3D}/l_{\rm ho}) = -0.730, -2.55, -4.34, \ldots$ in the $m = 0$ channel, $\sqrt{m_B/m_{AB}}(a_{\rm 3D}/l_{\rm ho}) = -1.96, -3.69, -5.44, \ldots$ in the $m = 1$ channel, $\sqrt{m_B/m_{AB}}(a_{\rm 3D}/l_{\rm ho}) = -3.14, -4.85, -6.58, \ldots$ in the $m = 2$ channel, and $\sqrt{m_B/m_{AB}}(a_{\rm 3D}/l_{\rm ho}) = -4.31, -6.00, -7.72, \ldots$ in the $m = 3$ channel.

IV. 2D-3D MIXED DIMENSIONS

A. Scattering theory [35]

The scattering of a quasi-2D A atom with a B atom in 3D is described by a Schrödinger equation,

$$\begin{aligned} & \left(-\frac{\nabla_{z_A}^2}{2m_A} + \frac{1}{2}m_A\omega^2 z_A^2 - \frac{\nabla_{z_B}^2}{2m_B} - \frac{\nabla_{\boldsymbol{\rho}_{AB}}^2}{2m_{AB}} \right) \psi(z_A, z_B, \boldsymbol{\rho}_{AB}) \\ & = E\psi(z_A, z_B, \boldsymbol{\rho}_{AB}) \end{aligned} \tag{64}$$

for $\sqrt{(z_A - z_B)^2 + \boldsymbol{\rho}_{AB}^2} > 0$, where $\boldsymbol{\rho}_{AB} \equiv (x_A - x_B, y_A - y_B)$ and the center-of-mass motions in the x and y directions are eliminated. The short-range interspecies interaction

is implemented by the generalized Bethe-Peierls boundary condition [28,29]:

$$\psi(z_A,z_B,\boldsymbol{\rho}_{AB})\big|_{z_A,z_B\to z;\boldsymbol{\rho}_{AB}\to\mathbf{0}} \to \left[\frac{1}{\tilde{a}(\hat{E}_c)} - \frac{1}{\sqrt{(z_A-z_B)^2+\boldsymbol{\rho}_{AB}^2}}\right]\chi(z). \quad (65)$$

The collision energy operator $\hat{E}_c$ in Eq. (6) in the present case is given by

$$\hat{E}_c = E - \left(-\frac{\nabla_z^2}{2M} + \frac{1}{2}m_A\omega^2 z^2\right). \quad (66)$$

The solution to the Schrödinger equation (64) can be written as

$$\psi(z_A,z_B,\boldsymbol{\rho}_{AB}) = \psi_0(z_A,z_B,\boldsymbol{\rho}_{AB}) + \frac{2\pi}{m_{AB}}\int dz' G_E(z_A,z_B,\boldsymbol{\rho}_{AB};z',z',\mathbf{0})\chi(z'), \quad (67)$$

where ψ_0 is a solution in the noninteracting limit and G_E is the retarded Green's function for the noninteracting Hamiltonian:

$$\begin{aligned} G_E(z_A,z_B,\boldsymbol{\rho}_{AB};z'_A,z'_B,\boldsymbol{\rho}'_{AB}) &\equiv \langle z_A,z_B,\boldsymbol{\rho}_{AB}|\frac{1}{E-H_0+i0^+}|z'_A,z'_B,\boldsymbol{\rho}'_{AB}\rangle \\ &= -\frac{m_{AB}}{2\pi}\sum_{n_z}\phi_{n_z}(z_A)\phi^*_{n_z}(z'_A) \\ &\times \frac{e^{-\sqrt{2m_B}\sqrt{(n_z+\frac{1}{2})\omega-E-i0^+}|\tilde{\boldsymbol{r}}_B-\tilde{\boldsymbol{r}}'_B|}}{|\tilde{\boldsymbol{r}}_B-\tilde{\boldsymbol{r}}'_B|}. \end{aligned} \quad (68)$$

Here ϕ_{n_z} is the normalized wave function of an A atom in the 1D harmonic potential, and $\tilde{\boldsymbol{r}}_B \equiv (-\sqrt{\frac{m_{AB}}{m_B}}\boldsymbol{\rho}_{AB}, z_B)$ are coordinates of the B atom relative to the confined A atom. The anisotropic factor is such because a separation in the z direction is associated with m_B while separations in the x and y directions are associated with m_{AB} [see the last two terms in Eq. (64)].

We now consider the low-energy scattering in which

$$E - \frac{1}{2}\omega \equiv \frac{k^2}{2m_B} \ll \omega \quad (69)$$

is satisfied, and then ψ_0 becomes

$$\psi_0(z_A,z_B,\boldsymbol{\rho}_{AB}) = Ce^{i\boldsymbol{k}\cdot\tilde{\boldsymbol{r}}_B}\phi_0(z_A), \quad (70)$$

which represents the A atom in the ground state of the 1D harmonic potential and the plane wave of B atom with the wave vector $\boldsymbol{k}$. The asymptotic form of the wave function at a large distance $|\tilde{\boldsymbol{r}}_B| \gg l_{\rm ho}$ is given by

$$\psi(z_A,z_B,\boldsymbol{\rho}_{AB}) \to C\left[e^{i\boldsymbol{k}\cdot\tilde{\boldsymbol{r}}_B} + \frac{e^{ik\tilde{r}_B}}{\tilde{r}_B}f(k_z,k'_z)\right]\phi_0(z_A), \quad (71)$$

where $f(k_z,k'_z)$ with $\boldsymbol{k}' \equiv k\hat{\tilde{\boldsymbol{r}}}_B$ defines the two-body scattering amplitude in the 2D-3D mixed dimensions:

$$f(k_z,k'_z) \equiv -\frac{1}{C}\int dz' e^{-ik'_z z'}\phi^*_0(z')\chi(z'). \quad (72)$$

We note that χ has an implicit k_z dependence and both χ and f depend on k through the Green's function (68).

The unknown function χ can be determined by substituting the solution (67) into the Bethe-Peierls boundary condition (65). Defining the regular part of the Green's function $\mathcal{G}$ by

$$G_E(z_A,z_B,\boldsymbol{\rho}_{AB};z',z',\mathbf{0})|_{z_A,z_B\to z;\boldsymbol{\rho}_{AB}\to\mathbf{0}} \equiv -\frac{m_{AB}}{2\pi\sqrt{(z_A-z_B)^2+\boldsymbol{\rho}_{AB}^2}}\delta(z-z') + \mathcal{G}(z;z'), \quad (73)$$

we obtain

$$\frac{1}{\tilde{a}(\hat{E}_c)}\chi(z) = Ce^{ik_z z}\phi_0(z) + \frac{2\pi}{m_{AB}}\int dz'\mathcal{G}(z;z')\chi(z'). \quad (74)$$

This integral equation determines χ/C, which in turn provides f from Eq. (72).

Because the system has a reflection symmetry about the z axis, f, χ, and $\mathcal{G}$ can be decomposed into their even- and odd-parity components:

$$f_\pm(k_z,k'_z) = \frac{f(k_z,k'_z) \pm f(k_z,-k'_z)}{2}, \quad (75)$$

$$\chi_\pm(z) = \frac{\chi(z)\pm\chi(-z)}{2}, \quad (76)$$

$$\mathcal{G}_\pm(z;z') = \frac{\mathcal{G}(z;z')\pm\mathcal{G}(z;-z')}{2}. \quad (77)$$

Equations (72) and (74) lead to the even- and odd-parity scattering amplitudes given by

$$f_\pm(k_z,k'_z) = -\frac{1}{C}\int dz'\frac{e^{-ik'_z z'} \pm e^{ik'_z z'}}{2}\phi^*_0(z')\chi_\pm(z') \quad (78)$$

with

$$\frac{1}{\tilde{a}(\hat{E}_c)}\chi_\pm(z) = C\frac{e^{ik_z z} \pm e^{-ik_z z}}{2}\phi_0(z) + \frac{2\pi}{m_{AB}}\int dz'\mathcal{G}_\pm(z;z')\chi_\pm(z'). \quad (79)$$

From the explicit calculation that uses the Green's function in Eq. (68), we can show that $f_\pm$ has the following low-energy expansion:

$$\lim_{k\to0} f_+(k_z,k'_z) = -\frac{1}{\frac{1}{a^{(+)}_{\rm eff}} - \frac{1}{2}r^{(+)}_{\rm eff}k^2 + O(k^4) + ik[1+O(k^2)]} + O\left(k_z^2,k_z'^2\right) \quad (80)$$

and

$$\lim_{k\to0} f_-(k_z,k'_z) = -\frac{3k_z k'_z}{\frac{1}{a^{(-)}_{\rm eff}} - \frac{1}{2}r^{(-)}_{\rm eff}k^2 + O(k^4) + ik^3[1+O(k^2)]} + O\left(k_z^3k'_z,k_zk_z'^3\right), \quad (81)$$

where $a^{(\pm)}_{\rm eff}$ and $r^{(\pm)}_{\rm eff}$ are effective scattering "length" and "range" parameters in the even- and odd-parity channels. Note that $a^{(\pm)}_{\rm eff}$ has the dimension of (length)$^{2\mp1}$ and $r^{(\pm)}_{\rm eff}$ has (length)$^{\pm1}$. This unusual form of the low-energy expansion is owing to the lack of full 3D rotational symmetries.

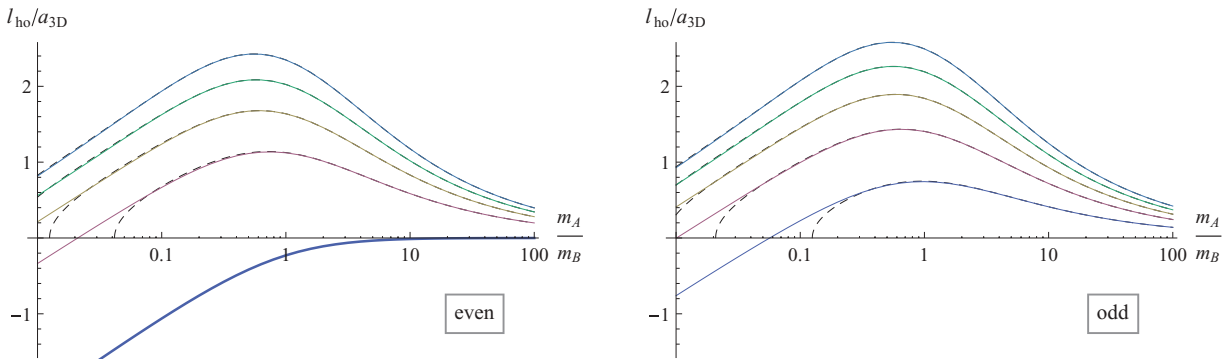

FIG. 6. (Color online) 2D-3D mixture: Positions of the lowest five resonances in terms of l_{ho}/a_{3D} for even-parity (left) and odd-parity (right) channels as functions of the mass ratio m_A/m_B. The dashed curves are from the approximate formula $E_{AB} = \frac{1}{2}\hbar\omega$ by using Eq. (3) with $E_b = -\hbar^2/(2m_{AB}a_{3D}^2)$.

Substituting the expansion of $f_\pm$ into Eq. (78), we can determine the low-energy scattering parameters. In particular, the effective scattering length $a_{\rm eff}^{(\pm)}$ is given by

$$\frac{1}{\tilde{a}(\hat{E}_c)}\chi_+(z) = \frac{1}{a_{\rm eff}^{(+)}}\phi_0(z)\int dz'\phi_0^*(z')\chi_+(z') + \frac{2\pi}{m_{AB}}\int dz'\mathcal{G}_+(z;z')\Big|_{k\to 0}\chi_+(z') \quad (82)$$

and

$$\frac{1}{\tilde{a}(\hat{E}_c)}\chi_-(z) = \frac{1}{3a_{\rm eff}^{(-)}}z\phi_0(z)\int dz'z'\phi_0^*(z')\chi_-(z') + \frac{2\pi}{m_{AB}}\int dz'\mathcal{G}_-(z;z')\Big|_{k\to 0}\chi_-(z'), \quad (83)$$

where we have eliminated C. The even- and odd-parity resonances in the 2D-3D mixed dimensions are defined by the divergence of $a_{\rm eff}^{(\pm)} \to \infty$, which occurs when

$$\frac{1}{\tilde{a}(\hat{E}_c)}\chi_\pm(z) = \frac{2\pi}{m_{AB}}\int dz'\mathcal{G}_\pm(z;z')\Big|_{k\to 0}\chi_\pm(z') \quad (84)$$

is satisfied.

B. Positions of resonances

We now solve the integral equation (84) numerically to determine the positions of even- and odd-parity resonances. For the purpose of illustrating qualitative results, we shall set $r_{3D} = 0$. For quantitative predictions in a specific atomic mixture, it is necessary but straightforward to include the effective range correction [27]. Some details of our method to solve the integral equation are shown in Appendix C.

Figure 6 shows the positions of the lowest five resonances in terms of l_{ho}/a_{3D} for even- and odd-parity channels as functions of the mass ratio m_A/m_B. For completeness, we have included the result for the even-parity resonance, which has been reported in Ref. [24]. As we have discussed in Sec. I, there exists a series of resonances in each parity channel induced from the purely s-wave interaction in a free space. Indeed, the resonance positions are well described by the approximate formula $E_{AB} = \frac{1}{2}\hbar\omega$ by using Eq. (3) with $E_b = -\hbar^2/(2m_{AB}a_{3D}^2)$ in a wide range of the mass ratio $m_A/m_B \gtrsim 1$.

C. Confinement-induced molecules

On the $a_{\rm eff}^{(\pm)} > 0$ side of every resonance, a shallow AB molecule is formed. In the vicinity of the resonance $a_{\rm eff}^{(\pm)} \gg l_{ho}^{2\mp1}$, its binding energy $\varepsilon_{AB} \equiv E - \frac{1}{2}\omega < 0$ is determined by the pole of the scattering amplitude [Eqs. (80) and (81)] with keeping the two dominant terms at $k \to 0$:

$$\varepsilon_{AB} = \begin{cases} -\dfrac{1}{2m_B a_{\rm eff}^{(+)2}} & \text{for even parity,} \\ \dfrac{1}{m_B a_{\rm eff}^{(-)} r_{\rm eff}^{(-)}} & \text{for odd parity.} \end{cases} \quad (85)$$

Away from the resonance, these universal formulas are no longer valid. The binding energy $\varepsilon_{AB} = -\kappa^2/(2m_B)$ has to be determined by solving the integral equation

$$\frac{1}{\tilde{a}(\hat{E}_c)}\chi_\pm(z) = \frac{2\pi}{m_{AB}}\int dz'\mathcal{G}_\pm(z;z')\Big|_{k\to i\kappa}\chi_\pm(z'). \quad (86)$$

We now derive the asymptotic form of the molecular wave function in the vicinity of the even- or odd-parity resonance where $l_{ho} \ll \kappa^{-1} \ll |\tilde{\boldsymbol{r}}_B|$ is satisfied. From Eqs. (67) and (68) with the replacement $k \to i\kappa$, we find

$$\psi(z_A,z_B,\boldsymbol{\rho}_{AB}) \to -\sum_{\ell=\text{even or odd}}^{\infty}\sqrt{\frac{4\pi}{2\ell+1}}\frac{e^{-\kappa\tilde{r}_B}}{\tilde{r}_B^{\ell+1}}\phi_0(z_A) \times Y_\ell^0(\hat{\tilde{\boldsymbol{r}}}_B)\int dz'|z'|^\ell\phi_0^*(z')\chi_\pm(z'). \quad (87)$$

One can see that different spherical harmonics $\sim Y_\ell^0$ contribute owing to the lack of full 3D rotational symmetries. The s-wave nature of the free-space interaction ensures that only the $m = 0$ component contributes so that the wave function is independent of $\hat{\boldsymbol{\rho}}_{AB}$. The asymptotic behavior at a large separation $|\tilde{\boldsymbol{r}}_B| \to \infty$ is dominated by the $\ell = 0$ or 1 component in the even- or odd-parity channel, respectively. Therefore, we can phrase the even (odd)-parity resonance as an s-wave (p-wave) resonance in the 2D-3D mixture. The angular part of the asymptotic wave function of a shallow p-wave molecule $\psi \sim Y_1^0(\hat{\tilde{\boldsymbol{r}}}_B)$ is illustrated in Fig. 1.

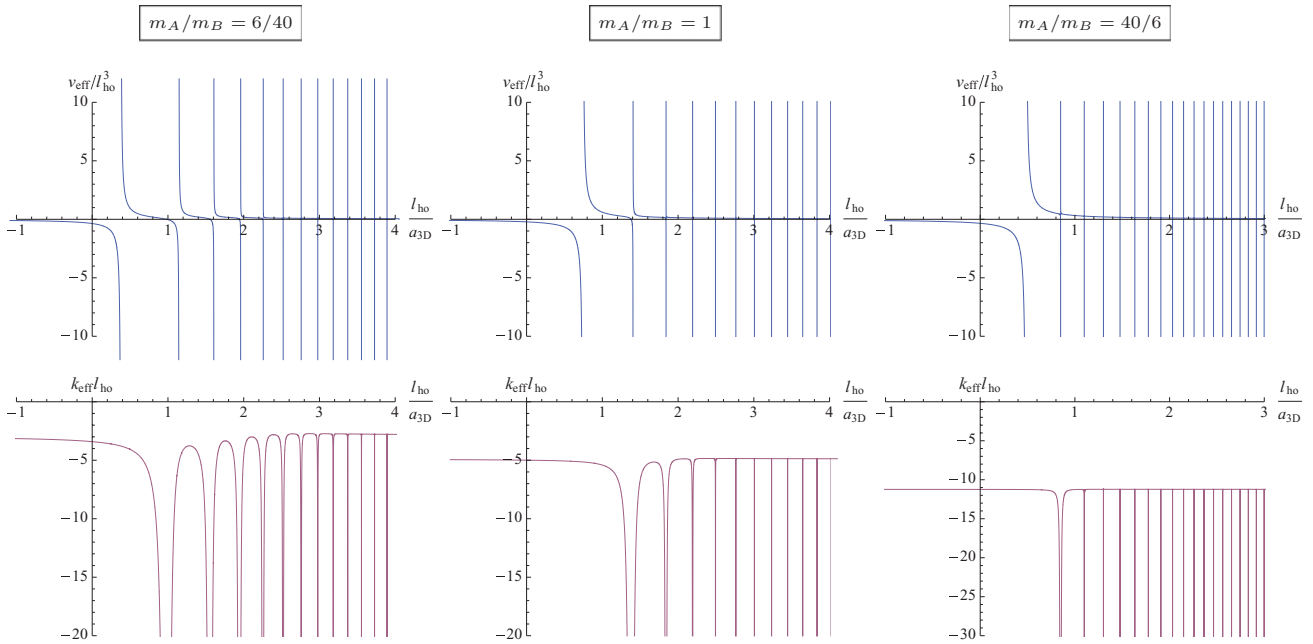

FIG. 7. (Color online) 2D-3D mixture: p-wave effective scattering volume $v_{\rm eff}/l_{\rm ho}^3$ (upper figures) and effective momentum $k_{\rm eff} l_{\rm ho}$ (lower figures) as functions of $l_{\rm ho}/a_{\rm 3D}$ for mass ratios $m_A/m_B = 6/40$ (left), 1 (middle), and 40/6 (right).

D. Scattering parameters in the p-wave channel

The effective scattering length in the s-wave (even-parity) channel $a_{\rm eff} \equiv a_{\rm eff}^{(+)}$ has been computed in Ref. [24]. Here we focus on the p-wave (odd-parity) channel and determine its two low-energy scattering parameters, namely, the effective scattering volume $v_{\rm eff} \equiv a_{\rm eff}^{(-)}$ and the effective momentum $k_{\rm eff} \equiv r_{\rm eff}^{(-)}$. The effective scattering volume can be computed by solving the integral equation (83) numerically (see Appendix C for details). In Fig. 7, $v_{\rm eff}/l_{\rm ho}^3$ for $r_{\rm 3D} = 0$ is plotted as a function of $l_{\rm ho}/a_{\rm 3D}$ for three mass ratios $m_A/m_B = 6/40$, 1, and 40/6. We confirm the existence of a series of p-wave resonances ($v_{\rm eff} \to \infty$) induced from the purely s-wave interaction in a free space, while they become narrower for larger $l_{\rm ho}/a_{\rm 3D}$. We also find that the resonance is wider when a lighter atom is confined in lower dimensions.

Similarly, the effective momentum can be computed from Eq. (78), and $k_{\rm eff} l_{\rm ho}$ for $r_{\rm 3D} = 0$ is plotted in Fig. 7 as a function of $l_{\rm ho}/a_{\rm 3D}$ for the same three mass ratios. In the vicinity of the p-wave resonance $v_{\rm eff} \gg l_{\rm ho}^3$, $v_{\rm eff}$ and $k_{\rm eff}$ determine the binding energy of a shallow p-wave molecule via the universal formula (85). Both $v_{\rm eff}$ and $k_{\rm eff}$ are important to the low-energy effective theory of the p-wave resonance discussed below.

E. Low-energy effective theory

The low-energy effective theory of the p-wave resonance in the 2D-3D mixed dimensions is provided by the action

$$
\begin{aligned}
S = & \int dt d\boldsymbol{\rho} \Psi_A^\dagger(t,\boldsymbol{\rho}) \left(i\partial_t + \frac{\nabla_{\boldsymbol{\rho}}^2}{2m_A} \right) \Psi_A(t,\boldsymbol{\rho}) \\
& + \int dt d\boldsymbol{\rho} dz \Psi_B^\dagger(t,\boldsymbol{\rho},z) \left(i\partial_t + \frac{\nabla_{\boldsymbol{\rho}}^2 + \nabla_z^2}{2m_B} \right) \Psi_B(t,\boldsymbol{\rho},z) \\
& + \int dt d\boldsymbol{\rho} \Phi^\dagger(t,\boldsymbol{\rho}) \left(i\partial_t + \frac{\nabla_{\boldsymbol{\rho}}^2}{2M} + \varepsilon_0 \right) \Phi(t,\boldsymbol{\rho}) \\
& + g_0 \int dt d\boldsymbol{\rho} [\Psi_A^\dagger(t,\boldsymbol{\rho}) \nabla_z \Psi_B^\dagger(t,\boldsymbol{\rho},0) \Phi(t,\boldsymbol{\rho}) \\
& + \Phi^\dagger(t,\boldsymbol{\rho}) \nabla_z \Psi_B(t,\boldsymbol{\rho},0) \Psi_A(t,\boldsymbol{\rho})]. \qquad (88)
\end{aligned}
$$

Ψ_A and Ψ_B fields represent the A and B atoms in 2D and 3D, respectively. The interaction between A and B atoms is described through their coupling with a p-wave molecular field Φ. g_0 is their coupling strength and ε_0 is the detuning from the resonance. These cutoff (Λ)-dependent bare parameters can be related to the effective scattering volume $v_{\rm eff}$ and effective momentum $k_{\rm eff}$ by matching the two-body scattering amplitude from the action (88) with that shown in Eqs. (75) and (81).

The standard diagrammatic calculation leads to the following scattering amplitude with collision energy $\varepsilon = k^2/(2m_B)$:

$$
i\mathcal{A}(k) = -\frac{ik_z k_z'}{\frac{k^2/(2m_B)+\varepsilon_0}{g_0^2} + \frac{m_{AB}}{3\pi^2}\left(\frac{\Lambda^3}{3} + \Lambda k^2 + \frac{\pi}{2} ik^3\right)}. \qquad (89)
$$

By defining

$$
\frac{\varepsilon_0}{g_0^2} + \frac{m_{AB}}{3\pi^2}\frac{\Lambda^3}{3} \equiv \frac{m_{AB}}{6\pi}\frac{1}{v_{\rm eff}} \qquad (90)
$$

and

$$
\frac{1}{2m_B g_0^2} + \frac{m_{AB}}{3\pi^2}\Lambda \equiv -\frac{m_{AB}}{6\pi}\frac{k_{\rm eff}}{2}, \qquad (91)
$$

we reproduce the scattering amplitude (81) in the p-wave (odd-parity) channel up to a kinematical factor:

$$
\mathcal{A}(k) = -\frac{2\pi}{m_{AB}} \frac{3k_z k_z'}{\frac{1}{v_{\rm eff}} - \frac{k_{\rm eff}}{2}k^2 + ik^3}. \qquad (92)
$$

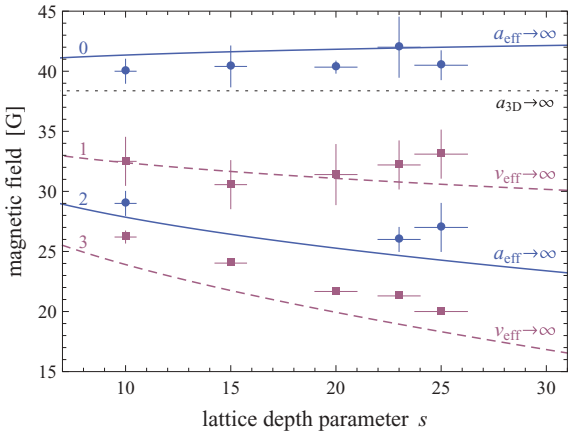

FIG. 8. (Color online) Experimentally measured resonance positions in terms of the magnetic field B as functions of the depth parameter s of an optical lattice [27]. Also shown are the predicted positions of s-wave ($a_{\rm eff}\to\infty$; solid curves) and p-wave ($v_{\rm eff}\to\infty$; dashed curves) resonances in a harmonic potential as well as the resonance position in a free space ($a_{\rm 3D}\to\infty$; dotted line).

This low-energy effective theory can be generalized easily to the case with more than one layer where B atoms are confined and could be used to investigate the many-body physics across the p-wave resonance as in the 3D case [31]. We note that the low-energy effective theory of the s-wave resonance in the 2D-3D mixed dimensions has been derived and used to study many-body problems in Refs. [37] and [38].

F. Comparison to experiment [27]

Finally, we compare our predictions to the experimental measurement of resonance positions reported in Ref. [27]. The Florence group has realized the 2D-3D mixed dimensions by using a Bose-Bose mixture of $A = {}^{41}$K and $B = {}^{87}$Rb with a species-selective 1D optical lattice:

$$V(z_A) = s\frac{k_L^2}{2m_A}\sin^2(k_L z_A). \tag{93}$$

Here s is the lattice depth parameter and $k_L = 2\pi/\lambda_L$ with $\lambda_L = 790.02$ nm is the wave vector of the laser light. By monitoring three-body inelastic losses, a series of resonances has been observed as a function of the magnetic field. The measured resonance positions are shown in Fig. 8 for five values of the lattice depth parameter, $s = 10,15,20,23,$ and 25.

As for theoretical predictions, we assume that the lattice potential (93) can be approximated by a harmonic potential:

$$V(z_A) \approx s\frac{k_L^4}{2m_A}z_A^2 \equiv \frac{1}{2}m_A\omega^2 z_A^2. \tag{94}$$

The harmonic oscillator length is given from the laser wavelength by $l_{\rm ho} = \lambda_L/(2\pi s^{1/4})$. With the use of the free-space value of the effective range $r_{\rm 3D} = 168.37a_0$ for the ^{41}K-^{87}Rb mixture, we solve the integral equation (84) numerically to determine the resonance positions in terms of $l_{\rm ho}/a_{\rm 3D}$. The free-space scattering length $a_{\rm 3D}$ thus obtained is converted into the magnetic field B (G) by the following empirical formula [27]:

$$\frac{a_{\rm 3D}}{a_0} = 208\left(1 + \frac{30.9}{B+38.52} - \frac{49.92}{B-38.37} - \frac{1.64}{B-78.67}\right), \tag{95}$$

where a_0 is the Bohr radius and the resonance in a free space occurs at $B = 38.4$ G. These critical magnetic field values for the s-wave ($a_{\rm eff}\to\infty$) and p-wave ($v_{\rm eff}\to\infty$) resonances are plotted in Fig. 8 as functions of the lattice depth parameter s.

In Fig. 8, the resonances are labeled by an integer $n = 0,1,2,3$ in descending order, corresponding to n in Eq. (3). One can see the reasonable agreement between the experimental measurements and the theoretical predictions for $n = 0$ (s-wave) and $n = 1$ (p-wave) resonances. They begin to deviate for larger n simply because the harmonic potential approximation (94) becomes worse for higher excited states in an optical lattice. Although the lattice potential (93) has to be taken into account to improve the quantitative agreement [27], for a sufficiently strong optical lattice, the resonances corresponding to odd n should be the p-wave resonances in the 2D-3D mixed dimensions, as we have discussed in this section. Further experimental investigations to confirm the p-wave nature of these resonances would be worthwhile. The p-wave nature of shallow molecules as illustrated in Fig. 1 could be seen as a suppression of the density of B atoms, as opposed to an enhancement for s-wave molecules, at the center of the confinement potential after a sudden change of $v_{\rm eff} > 0$ to its negative side.

V. SUMMARY AND CONCLUDING REMARKS

In this paper, we showed that a purely s-wave interaction in a free space can induce higher partial-wave resonances in mixed dimensions. We developed two-body scattering theories in all three cases of 0D-3D, 1D-3D, and 2D-3D mixtures, and determined the positions of higher partial-wave resonances in terms of the free-space scattering length, assuming a harmonic confinement potential. We also computed the low-energy scattering parameters in the p-wave channel (effective scattering volume and momentum) that are necessary for the low-energy effective theory of the p-wave resonance. Potentially our study paves the way for a variety of physics, such as Anderson localization of matter waves under p-wave resonant scatterers in the 0D-3D mixed dimensions [23,39,40], Shiba bound states in a superfluid medium [34], and Bose-Einstein condensation of p-wave molecules in the 2D-3D mixed dimensions, provided that such molecules are long lived.

When both A and B atoms are fermionic (such as for the ^{6}Li-^{40}K mixture [41–45]), inelastic three-body, atom-molecule, and molecule-molecule collisions decaying into deeply bound dimers whose size is set by the range of interatomic potential r_0 are suppressed. This is because at a short distance $\sim r_0 \ll l_{\rm ho}$, the confinement potential is irrelevant, and in the s-wave interspecies interaction the Pauli exclusion principle is effective to suppress the inelastic collisions decaying into the deeply bound dimers [22]. An order-of-magnitude estimate of such a three-body recombination rate can be found in Refs. [36]

and [29] for wide Feshbach resonances and in Ref. [29] for narrow Feshbach resonances.

Therefore, for a Fermi-Fermi mixture in mixed dimensions, the relaxation of molecules is dominated by the decay into deeper molecular states of size $\sim l_{\rm ho}$ if they exist. In the vicinity of the s-wave resonance at the smallest value of $l_{\rm ho}/a_{\rm 3D}$, indicated by thick curves in Figs. 2, 4, and 6 , there is no such molecular state and thus associated s-wave molecules are long lived. However, in the vicinity of the higher partial-wave resonances, there is always at least one deeper molecular state. The inelastic atom-molecule and molecule-molecule collisions decaying into such molecular states are not generally suppressed, and thus p-wave or higher partial-wave molecules in mixed dimensions would be short lived. It is therefore an important future problem to investigate as to whether the inelastic collisions of p-wave molecules decaying into the lowest s-wave state of size $\sim l_{\rm ho}$ could be suppressed, for example, by controlling the system parameters.

We conclude this paper by discussing a simple analogy between a tower of our confinement-induced molecules and Kaluza-Klein modes in extra-dimension models [46]. Suppose our 3D world has one compact extra dimension with an extent of L. Then the momentum of a 4D particle in the extra fourth direction is quantized as $p_4 = 2\pi\hbar n/L$. Because we live in 3D, such a particle can be viewed as a tower of "new particles" with the quantized masses $m_n = 2\pi\hbar n/cL$. These new particles are called Kaluza-Klein modes and could be observed by colliding high-energy particles $> 2\pi\hbar c/L$ at the Large Hadron Collider.

Now in our case, for example, in the 2D-3D mixed dimensions, the motion of a 3D molecule in the "extra" z direction is quantized as in Eq. (3) because of the confinement potential. We can view such quantized energy levels as a tower of new "Feshbach molecules" analogous to the Kaluza-Klein modes. Unlike in extra-dimension models, our particle is a composite molecule and we can control its binding energy to shift the energies of the tower of new molecules. When each of them crosses the scattering threshold, the resonance occurs. A series of such resonances caused by the "Kaluza-Klein" tower of confinement-induced molecules has been investigated in this paper and observed in the cold-atom experiment [24,27].

ACKNOWLEDGMENTS

The authors thank Yvan Castin, Eugene Demler, David Pekker, Andrey Turlapov, Fa Wang, Zhenhua Yu, and Martin Zwierlein for valuable discussions and Jacopo Catani, Giacomo Lamporesi, and Francesco Minardi for providing the experimental data. Y.N. was supported by MIT Department of Physics Pappalardo Program and the DOE Office of Nuclear Physics under Grant No. DE-FG02-94ER40818. S.T. thanks the Institute for Advanced Study in Tsinghua University for hospitality when this work was near completion.

APPENDIX A: 0D-3D MIXED DIMENSIONS

Here we present some details of our method to solve integral equations derived in Sec. II. The central issue is the evaluation of the regular part of the Green's function defined in Eq. (14). When $E - \frac{3}{2}\omega \equiv \frac{k^2}{2m_B} \leqslant 0$, it is useful to represent $\mathcal{G}$ as

$$\mathcal{G}(\boldsymbol{r};\boldsymbol{r}') = -\int_0^\infty d\tau e^{\frac{k^2}{2m_B}\tau}\left(\frac{m_A\omega e^{\omega\tau}}{2\pi\sinh\omega\tau}\right)^{3/2}\left(\frac{m_B}{2\pi\tau}\right)^{3/2}\exp\left[-\frac{m_A\omega}{2}\frac{(\boldsymbol{r}+\boldsymbol{r}')^2\cosh\omega\tau - 2\boldsymbol{r}\cdot\boldsymbol{r}'}{\sinh\omega\tau} - \frac{m_B}{2\tau}(\boldsymbol{r}-\boldsymbol{r}')^2\right] + \int_0^\infty d\tau\left(\frac{m_{AB}}{2\pi\tau}\right)^{3/2}\delta(\boldsymbol{r}-\boldsymbol{r}'). \tag{A1}$$

Its partial-wave projection gives

$$\begin{aligned}\mathcal{G}_\ell(r;r') &\equiv \frac{1}{2}\int_{-1}^{1} d\cos\theta\,\mathcal{G}(\boldsymbol{r};\boldsymbol{r}')P_\ell(\cos\theta)\\ &= -\int_0^\infty d\tau e^{\frac{k^2}{2m_B}\tau}\left(\frac{m_A\omega e^{\omega\tau}}{2\pi\sinh\omega\tau}\right)^{3/2}\left(\frac{m_B}{2\pi\tau}\right)^{3/2} i^{-l} j_l\left[i\left(\frac{m_A\omega}{\sinh\omega\tau}+\frac{m_B}{\tau}\right)rr'\right]\\ &\quad\times\exp\left[-\left(\frac{m_A\omega\cosh\omega\tau}{\sinh\omega\tau}+\frac{m_B}{\tau}\right)\frac{r^2+r'^2}{2}\right] + \int_0^\infty d\tau\left(\frac{m_{AB}}{2\pi\tau}\right)^{3/2}\frac{\delta(r-r')}{4\pi r^2}.\end{aligned} \tag{A2}$$

We now evaluate the matrix elements of $\mathcal{G}_\ell$ with respect to the eigenfunctions of 3D harmonic oscillator with orbital angular momentum ℓ:

$$\phi_n^{(\ell)}(r) \equiv \frac{1}{l_{\rm ho}^{3/2}}\sqrt{\frac{n!}{2\pi\left(n+\ell+\frac{1}{2}\right)!}}e^{-r^2/(2l_{\rm ho}^2)}\left(\frac{r}{l_{\rm ho}}\right)^\ell L_n^{(\ell+\frac{1}{2})}(r^2/l_{\rm ho}^2), \tag{A3}$$

which form an orthonormal basis:

$$\int d\boldsymbol{r}\phi_n^{(\ell)}(r)\phi_{n'}^{(\ell)}(r) = \int_0^\infty 4\pi r^2 dr\phi_n^{(\ell)}(r)\phi_{n'}^{(\ell)}(r) = \delta_{nn'}. \tag{A4}$$

A lengthy but straightforward calculation leads to

$$M_{ij}^{(\ell)} \equiv \frac{2\pi l_{\rm ho}}{m_{AB}} \int d\boldsymbol{r} d\boldsymbol{r}' \phi_i^{(\ell)}(r) \mathcal{G}_\ell(r;r') \phi_j^{(\ell)}(r')$$
$$= \frac{-1}{4\sqrt{\pi}} \sqrt{\frac{m_B}{m_A}} \frac{m_B}{m_{AB}} \sqrt{\binom{i+l+\frac{1}{2}}{i}\binom{j+l+\frac{1}{2}}{j}} \int_0^\infty \frac{\omega d\tau}{(\omega\tau)^{3/2}} e^{\frac{k^2}{2m_B}\tau} \left(\frac{e^{\omega\tau}}{\sinh\omega\tau}\right)^{3/2} Y^l \left(\frac{1}{X^2-Y^2}\right)^{l+\frac{3}{2}}$$
$$\times \left(1-\frac{X}{X^2-Y^2}\right)^{i+j} {}_2F_1\left[-i,-j;l+\frac{3}{2};\left(\frac{Y}{X^2-X-Y^2}\right)^2\right] + \delta_{ij}\sqrt{\frac{m_{AB}}{2\pi m_A}} \int_0^\infty \frac{\omega d\tau}{(\omega\tau)^{3/2}}, \tag{A5}$$

where ${}_2F_1$ is the hypergeometric function and

$$X \equiv \frac{1}{2}\left(\frac{1}{\tanh\omega\tau} + \frac{m_B}{m_A\omega\tau} + 1\right) \quad \text{and} \quad Y \equiv \frac{1}{2}\left(\frac{1}{\sinh\omega\tau} + \frac{m_B}{m_A\omega\tau}\right). \tag{A6}$$

Expanding χ_ℓ in terms of $\phi_n^{(\ell)}$, the integral equations in Sec. II reduce to linear algebraic equations that have been solved numerically.

APPENDIX B: 1D-3D MIXED DIMENSIONS

Here we present some details of our method to solve integral equations derived in Sec. III. The central issue is the evaluation of the regular part of the Green's function defined in Eq. (44). When $E-\omega \equiv \frac{k^2}{2m_B} \leqslant 0$, it is useful to represent $\mathcal{G}$ as

$$\mathcal{G}(\boldsymbol{\rho};\boldsymbol{\rho}') = -\int_0^\infty d\tau e^{\frac{k^2}{2m_B}\tau} \frac{m_A\omega e^{\omega\tau}}{2\pi\sinh\omega\tau} \frac{m_B}{2\pi\tau} \sqrt{\frac{m_{AB}}{2\pi\tau}} \exp\left[-\frac{m_A\omega}{2}\frac{(\boldsymbol{\rho}+\boldsymbol{\rho}')^2\cosh\omega\tau - 2\boldsymbol{\rho}\cdot\boldsymbol{\rho}'}{\sinh\omega\tau} - \frac{m_B}{2\tau}(\boldsymbol{\rho}-\boldsymbol{\rho}')^2\right]$$
$$+ \int_0^\infty d\tau \left(\frac{m_{AB}}{2\pi\tau}\right)^{3/2} \delta(\boldsymbol{\rho}-\boldsymbol{\rho}'). \tag{B1}$$

Its partial-wave projection gives

$$\mathcal{G}_m(\rho;\rho') \equiv \frac{1}{\pi}\int_0^\pi d\varphi \mathcal{G}(\boldsymbol{\rho};\boldsymbol{\rho}')\cos(m\varphi)$$
$$= -\int_0^\infty d\tau e^{\frac{k^2}{2m_B}\tau} \frac{m_A\omega e^{\omega\tau}}{2\pi\sinh\omega\tau} \frac{m_B}{2\pi\tau} \sqrt{\frac{m_{AB}}{2\pi\tau}} I_m\left[\left(\frac{m_A\omega}{\sinh\omega\tau} + \frac{m_B}{\tau}\right)\rho\rho'\right]$$
$$\times \exp\left[-\left(\frac{m_A\omega\cosh\omega\tau}{\sinh\omega\tau} + \frac{m_B}{\tau}\right)\frac{\rho^2+\rho'^2}{2}\right] + \int_0^\infty d\tau \left(\frac{m_{AB}}{2\pi\tau}\right)^{3/2} \frac{\delta(\rho-\rho')}{2\pi\rho}. \tag{B2}$$

We now evaluate the matrix elements of $\mathcal{G}_m$ with respect to the eigenfunctions of 2D harmonic oscillator with magnetic quantum number m:

$$\phi_n^{(m)}(\rho) \equiv \frac{1}{l_{\rm ho}}\sqrt{\frac{n!}{\pi(n+m)!}} e^{-\rho^2/(2l_{\rm ho}^2)} \left(\frac{\rho}{l_{\rm ho}}\right)^m L_n^{(m)}(\rho^2/l_{\rm ho}^2), \tag{B3}$$

which form an orthonormal basis:

$$\int d\boldsymbol{\rho}\phi_n^{(m)}(\rho)\phi_{n'}^{(m)}(\rho) = \int_0^\infty 2\pi\rho d\rho \phi_n^{(m)}(\rho)\phi_{n'}^{(m)}(\rho) = \delta_{nn'}. \tag{B4}$$

A lengthy but straightforward calculation leads to

$$M_{ij}^{(m)} \equiv \frac{2\pi l_{\rm ho}}{m_{AB}} \int d\boldsymbol{\rho} d\boldsymbol{\rho}' \phi_i^{(m)}(\rho) \mathcal{G}_m(\rho;\rho') \phi_j^{(m)}(\rho')$$
$$= \frac{-1}{2\sqrt{2\pi}} \frac{m_B}{\sqrt{m_A m_{AB}}} \sqrt{\binom{i+m}{i}\binom{j+m}{j}} \int_0^\infty \frac{\omega d\tau}{(\omega\tau)^{3/2}} e^{\frac{k^2}{2m_B}\tau} \frac{e^{\omega\tau}}{\sinh\omega\tau} Y^m \left(\frac{1}{X^2-Y^2}\right)^{m+1}$$
$$\times \left(1-\frac{X}{X^2-Y^2}\right)^{i+j} {}_2F_1\left[-i,-j;m+1;\left(\frac{Y}{X^2-X-Y^2}\right)^2\right] + \delta_{ij}\sqrt{\frac{m_{AB}}{2\pi m_A}} \int_0^\infty \frac{\omega d\tau}{(\omega\tau)^{3/2}}. \tag{B5}$$

Expanding χ_m in terms of $\phi_n^{(m)}$, the integral equations in Sec. III reduce to linear algebraic equations that have been solved numerically.

APPENDIX C: 2D-3D MIXED DIMENSIONS

Here we present some details of our method to solve integral equations derived in Sec. IV. The central issue is the evaluation of the regular part of the Green's function defined in Eq. (73). When $E-\frac{1}{2}\omega \equiv \frac{k^2}{2m_B} \leqslant 0$, it is useful to represent $\mathcal{G}$ as

$$\mathcal{G}(z;z') = -\int_0^\infty d\tau e^{\frac{k^2}{2m_B}\tau}\sqrt{\frac{m_A\omega e^{\omega\tau}}{2\pi\sinh\omega\tau}}\sqrt{\frac{m_B}{2\pi\tau}}\frac{m_{AB}}{2\pi\tau}\exp\left[-\frac{m_A\omega}{2}\frac{(z+z')^2\cosh\omega\tau-2zz'}{\sinh\omega\tau}-\frac{m_B}{2\tau}(z-z')^2\right] + \int_0^\infty d\tau\left(\frac{m_{AB}}{2\pi\tau}\right)^{3/2}\delta(z-z'). \tag{C1}$$

Its parity projection gives

$$\begin{aligned}\mathcal{G}_\pm(z;z') &\equiv \frac{\mathcal{G}(z;z')\pm\mathcal{G}(z;-z')}{2}\\ &= -\int_0^\infty d\tau e^{\frac{k^2}{2m_B}\tau}\sqrt{\frac{m_A\omega e^{\omega\tau}}{2\pi\sinh\omega\tau}}\sqrt{\frac{m_B}{2\pi\tau}}\frac{m_{AB}}{2\pi\tau}\left\{\begin{matrix}\cosh\\ \sinh\end{matrix}\right\}\left[\left(\frac{m_A\omega}{\sinh\omega\tau}+\frac{m_B}{\tau}\right)zz'\right]\\ &\quad\times\exp\left[-\left(\frac{m_A\omega\cosh\omega\tau}{\sinh\omega\tau}+\frac{m_B}{\tau}\right)\frac{z^2+z'^2}{2}\right]+\int_0^\infty d\tau\left(\frac{m_{AB}}{2\pi\tau}\right)^{3/2}\frac{\delta(z-z')\pm\delta(z+z')}{2}.\end{aligned} \tag{C2}$$

We now evaluate the matrix elements of $\mathcal{G}_\pm$ with respect to the eigenfunctions of 1D harmonic oscillator:

$$\phi_n(z) \equiv \frac{1}{\sqrt{l_{\rm ho}}}\frac{\pi^{-1/4}}{\sqrt{2^n n!}}e^{-z^2/(2l_{\rm ho}^2)}H_n(z/l_{\rm ho}), \tag{C3}$$

which form an orthonormal basis:

$$\int dz\phi_n^*(z)\phi_{n'}(z) = \delta_{nn'}. \tag{C4}$$

A lengthy but straightforward calculation leads to

$$\begin{aligned}M_{ij}^{(+)} &\equiv \frac{2\pi l_{\rm ho}}{m_{AB}}\int dzdz'\phi_i(z)\mathcal{G}_+(z;z')\phi_j(z')\\ &= \frac{1}{2\sqrt{\pi}}\sqrt{\frac{m_B}{m_A}}\frac{(-1)^{\frac{i}{2}+\frac{j}{2}+1}}{(\frac{i}{2})!(\frac{j}{2})!}\sqrt{\frac{i!j!}{2^{i+j}}}\int_0^\infty\frac{\omega d\tau}{(\omega\tau)^{3/2}}e^{\frac{k^2}{2m_B}\tau}\sqrt{\frac{e^{\omega\tau}}{\sinh\omega\tau}}\left(\frac{1}{X^2-Y^2}\right)^{1/2}\\ &\quad\times\left(1-\frac{X}{X^2-Y^2}\right)^{\frac{i}{2}+\frac{j}{2}}{}_2F_1\left[-\frac{i}{2},-\frac{j}{2};\frac{1}{2};\left(\frac{Y}{X^2-X-Y^2}\right)^2\right]+\delta_{ij}\sqrt{\frac{m_{AB}}{2\pi m_A}}\int_0^\infty\frac{\omega d\tau}{(\omega\tau)^{3/2}}\end{aligned} \tag{C5}$$

for $i,j=$ even integers and

$$\begin{aligned}M_{ij}^{(-)} &\equiv \frac{2\pi l_{\rm ho}}{m_{AB}}\int dzdz'\phi_i(z)\mathcal{G}_-(z;z')\phi_j(z')\\ &= \frac{1}{\sqrt{\pi}}\sqrt{\frac{m_B}{m_A}}\frac{(-1)^{\frac{i}{2}+\frac{j}{2}}}{(\frac{i-1}{2})!(\frac{j-1}{2})!}\sqrt{\frac{i!j!}{2^{i+j}}}\int_0^\infty\frac{\omega d\tau}{(\omega\tau)^{3/2}}e^{\frac{k^2}{2m_B}\tau}\sqrt{\frac{e^{\omega\tau}}{\sinh\omega\tau}}Y\left(\frac{1}{X^2-Y^2}\right)^{3/2}\\ &\quad\times\left(1-\frac{X}{X^2-Y^2}\right)^{\frac{i}{2}+\frac{j}{2}-1}{}_2F_1\left[\frac{1-i}{2},\frac{1-j}{2};\frac{3}{2};\left(\frac{Y}{X^2-X-Y^2}\right)^2\right]+\delta_{ij}\sqrt{\frac{m_{AB}}{2\pi m_A}}\int_0^\infty\frac{\omega d\tau}{(\omega\tau)^{3/2}}\end{aligned} \tag{C6}$$

for $i,j=$ odd integers. Expanding $\chi_\pm$ in terms of ϕ_n, the integral equations in Sec. IV reduce to linear algebraic equations that have been solved numerically.

[1] C. Chin, R. Grimm, P. Julienne, and E. Tiesinga, Rev. Mod. Phys. **82**, 1225 (2010).

[2] W. Ketterle and M. W. Zwierlein, in *Proceedings of the International School of Physics "Enrico Fermi,"* edited by M. Inguscio, W. Ketterle, and C. Salomon (IOS, Amsterdam, 2008), and references therein.

[3] I. Bloch, J. Dalibard, and W. Zwerger, Rev. Mod. Phys. **80**, 885 (2008).

[4] S. Giorgini, L. P. Pitaevskii, and S. Stringari, Rev. Mod. Phys. **80**, 1215 (2008).

[5] T.-L. Ho and R. B. Diener, Phys. Rev. Lett. **94**, 090402 (2005).

[6] S. S. Botelho and C. A. R. Sá de Melo, J. Low Temp. Phys. **140**, 409 (2005).

[7] Y. Ohashi, Phys. Rev. Lett. **94**, 050403 (2005).

[8] V. Gurarie, L. Radzihovsky, and A. V. Andreev, Phys. Rev. Lett. **94**, 230403 (2005).

[9] C.-H. Cheng and S.-K. Yip, Phys. Rev. Lett. **95**, 070404 (2005); Phys. Rev. B **73**, 064517 (2006).
[10] C. A. Regal, C. Ticknor, J. L. Bohn, and D. S. Jin, Phys. Rev. Lett. **90**, 053201 (2003).
[11] J. Zhang, E. G. M. van Kempen, T. Bourdel, L. Khaykovich, J. Cubizolles, F. Chevy, M. Teichmann, L. Tarruell, S. J. J. M. F. Kokkelmans, and C. Salomon, Phys. Rev. A **70**, 030702(R) (2004).
[12] C. H. Schunck, M. W. Zwierlein, C. A. Stan, S. M. F. Raupach, W. Ketterle, A. Simoni, E. Tiesinga, C. J. Williams, and P. S. Julienne, Phys. Rev. A **71**, 045601 (2005).
[13] F. Chevy, E. G. M. van Kempen, T. Bourdel, J. Zhang, L. Khaykovich, M. Teichmann, L. Tarruell, S. J. J. M. F. Kokkelmans, and C. Salomon, Phys. Rev. A **71**, 062710 (2005).
[14] K. Günter, T. Stöferle, H. Moritz, M. Köhl, and T. Esslinger, Phys. Rev. Lett. **95**, 230401 (2005).
[15] J. P. Gaebler, J. T. Stewart, J. L. Bohn, and D. S. Jin, Phys. Rev. Lett. **98**, 200403 (2007).
[16] D. S. Jin, J. P. Gaebler, and J. T. Stewart, in *Proceedings of the International Conference on Laser Spectroscopy*, edited by L. Hollberg, J. Bergquist, and M. Kasevich (World Scientific, Singapore, 2008).
[17] J. Fuchs, C. Ticknor, P. Dyke, G. Veeravalli, E. Kuhnle, W. Rowlands, P. Hannaford, and C. J. Vale, Phys. Rev. A **77**, 053616 (2008).
[18] Y. Inada, M. Horikoshi, S. Nakajima, M. Kuwata-Gonokami, M. Ueda, and T. Mukaiyama, Phys. Rev. Lett. **101**, 100401 (2008).
[19] R. A. W. Maier, C. Marzok, C. Zimmermann, and Ph. W. Courteille, Phys. Rev. A **81**, 064701 (2010).
[20] J. Levinsen, N. R. Cooper, and V. Gurarie, Phys. Rev. Lett. **99**, 210402 (2007); Phys. Rev. A **78**, 063616 (2008).
[21] M. Jona-Lasinio, L. Pricoupenko, and Y. Castin, Phys. Rev. A **77**, 043611 (2008).
[22] D. S. Petrov, C. Salomon, and G. V. Shlyapnikov, Phys. Rev. Lett. **93**, 090404 (2004); Phys. Rev. A **71**, 012708 (2005); J. Phys. B **38**, S645 (2005).
[23] P. Massignan and Y. Castin, Phys. Rev. A **74**, 013616 (2006).
[24] Y. Nishida and S. Tan, Phys. Rev. Lett. **101**, 170401 (2008).
[25] L. J. LeBlanc and J. H. Thywissen, Phys. Rev. A **75**, 053612 (2007).
[26] J. Catani, G. Barontini, G. Lamporesi, F. Rabatti, G. Thalhammer, F. Minardi, S. Stringari, and M. Inguscio, Phys. Rev. Lett. **103**, 140401 (2009).
[27] G. Lamporesi, J. Catani, G. Barontini, Y. Nishida, M. Inguscio, and F. Minardi, Phys. Rev. Lett. **104**, 153202 (2010).
[28] D. S. Petrov, Phys. Rev. Lett. **93**, 143201 (2004).
[29] J. Levinsen, T. G. Tiecke, J. T. M. Walraven, and D. S. Petrov, Phys. Rev. Lett. **103**, 153202 (2009).
[30] See, for example, J. J. Sakurai, *Modern Quantum Mechanics* (Addison-Wesley, Reading, MA, 1994).
[31] V. Gurarie and L. Radzihovsky, Ann. Phys. **322**, 2 (2007).
[32] C. A. Bertulani, H. W. Hammer, and U. Van Kolck, Nucl. Phys. A **712**, 37 (2002).
[33] P. F. Bedaque, H. W. Hammer, and U. van Kolck, Phys. Lett. B **569**, 159 (2003).
[34] E. Vernier, D. Pekker, M. W. Zwierlein, and E. Demler, e-print arXiv:1010.6085 [cond-mat.quant-gas].
[35] In this paper, we use a different normalization of a_{eff} from that introduced in Ref. [24]. a_{eff} in this paper corresponds to $\sqrt{m_{AB}/m_B}a_{\text{eff}}$ in Ref. [24].
[36] Y. Nishida and S. Tan, Phys. Rev. A **79**, 060701(R) (2009).
[37] Y. Nishida, Ann. Phys. **324**, 897 (2009).
[38] Y. Nishida, Phys. Rev. A **82**, 011605 (2010).
[39] U. Gavish and Y. Castin, Phys. Rev. Lett. **95**, 020401 (2005).
[40] M. Antezza, Y. Castin, and D. A. W. Hutchinson, Phys. Rev. A **82**, 043602 (2010).
[41] M. Taglieber, A.-C. Voigt, T. Aoki, T. W. Hänsch, and K. Dieckmann, Phys. Rev. Lett. **100**, 010401 (2008).
[42] E. Wille *et al.*, Phys. Rev. Lett. **100**, 053201 (2008).
[43] A.-C. Voigt, M. Taglieber, L. Costa, T. Aoki, W. Wieser, T. W. Hänsch, and K. Dieckmann, Phys. Rev. Lett. **102**, 020405 (2009).
[44] T. G. Tiecke, M. R. Goosen, A. Ludewig, S. D. Gensemer, S. Kraft, S. J. J. M. F. Kokkelmans, and J. T. M. Walraven, Phys. Rev. Lett. **104**, 053202 (2010).
[45] D. Naik, A. Trenkwalder, C. Kohstall, F. M. Spiegelhalder, M. Zaccanti, G. Hendl, F. Schreck, R. Grimm, T. M. Hanna, and P. S. Julienne, e-print arXiv:1010.3662 [cond-mat.quant-gas].
[46] See, for example, R. Maartens and K. Koyama, Living Rev. Relativity **13**, 5 (2010).